



Dominant physical-biogeochemical drivers for the seasonal variations in the surface chlorophyll-a and subsurface chlorophyll-a maximum in the Bay of Bengal



K.M. Azam Chowdhury^{a,b,c}, Wensheng Jiang^{d,e,f,*}, Guimei Liu^c, Md. Kawser Ahmed^b, Shaila Akhter^{a,g}

^a College of Oceanic & Atmospheric Sciences, Ocean University of China, Qingdao 266100, China

^b Department of Oceanography & International Centre for Ocean Governance (ICOG), University of Dhaka, Dhaka 1000, Bangladesh

^c National Marine Environmental Forecasting Center, Beijing 100081, China

^d Physical Oceanography Laboratory/CIMST, Ocean University of China, Qingdao 266100, China

^e Qingdao National Laboratory for Marine Science and Technology, Qingdao 266100, China

^f Key laboratory of Marine Environment and Ecology, Ministry of Education, Ocean University of China, Qingdao, 266100, China

^g Bangladesh Betar, Ministry of Information and Broadcasting, Government of the People's Republic of Bangladesh, Dhaka 1207, Bangladesh

ARTICLE INFO

Article history:

Received 18 June 2020

Received in revised form 1 August 2021

Accepted 25 September 2021

Available online 29 September 2021

Keywords:

Bay of Bengal

Ekman pumping

Euphotic depth

Wind stress curl

Subsurface chlorophyll-a maximum

Depth of 26 °C isotherm

ABSTRACT

The seasonal variations and driving mechanisms of the surface and subsurface chlorophyll-a concentrations in the Bay of Bengal are far from resolved, as only a few local, short-term studies have been performed. Hence, this study investigates a comprehensive basin-wide framework of the seasonal variations in the chlorophyll-a concentration, its dominant external forcing, and the internal dynamics of the Bay of Bengal. Multivariate empirical orthogonal function decomposition and heterogeneous correlation analyses are applied to numerous observational, reanalysis, and satellite datasets, including chlorophyll-a, nutrients, temperature, salinity, turbidity, and wind stress curl datasets collected from various sources, including the Copernicus Marine Environment Monitoring Service, World Ocean Atlas, and ERA-Interim. This study suggests that the chlorophyll-a concentrations at both the surface and the subsurface chlorophyll-a maximum (SCM) are higher during summer and early autumn than during the other seasons, especially along the coastal regions and western part of the Bay of Bengal. During summer and early autumn, riverine nutrient inputs, the intrusion of nutritious water from the Arabian Sea, and coastal upwelling are the three dominant drivers controlling the chlorophyll-a concentrations at both the surface and the SCM. The positive wind stress curl-induced uplift of the thermocline increases the nutrient supply and thus significantly enhances the chlorophyll-a concentration at the SCM along the entire western side of the bay during the second half of the year. During spring, the deep euphotic depth plays a vital role in controlling the concentration and depth of the SCM. The depth of the 26 °C isotherm can be used as a proxy of the depth of the SCM. This study provides an improved understanding of the high chlorophyll-a concentrations and their drivers in five potential zones within the Bay of Bengal, which will help to identify the rich marine ecosystems therein.

© 2021 Elsevier B.V. All rights reserved.

1. Introduction

In the oligotrophic regions of the tropical and subtropical oceans, high subsurface chlorophyll-a concentrations appear just below the mixed layer (a layer with uniform density) and extend above the depth of the thermocline; this extent is defined as the subsurface chlorophyll-a layer (Fig. 1) (Furuya, 1990; Li

et al., 2012a; Thushara et al., 2019). Moreover, the maximum chlorophyll-a concentration (occurring at a given depth) within the subsurface chlorophyll-a layer is known as the subsurface chlorophyll-a maximum (SCM, see Fig. 1; Brown et al., 2015; Steiner et al., 2016). The SCM commonly forms near the bottom of the euphotic zone, the uppermost layer of the ocean that receives enough sunlight to support photosynthesis (Gong et al., 2017). Hence, the SCM is widely utilized as a proxy for the overall subsurface chlorophyll-a concentration in the oceans (Riley, 1949; Anderson, 1969; Fennel and Boss, 2003; Li et al., 2012a; Brown et al., 2015; Bhushan et al., 2018; Thushara et al.,

* Corresponding author at: Key laboratory of Marine Environment and Ecology, Ministry of Education, Ocean University of China, Qingdao, 266100, China.

E-mail address: wsjang@ouc.edu.cn (W. Jiang).

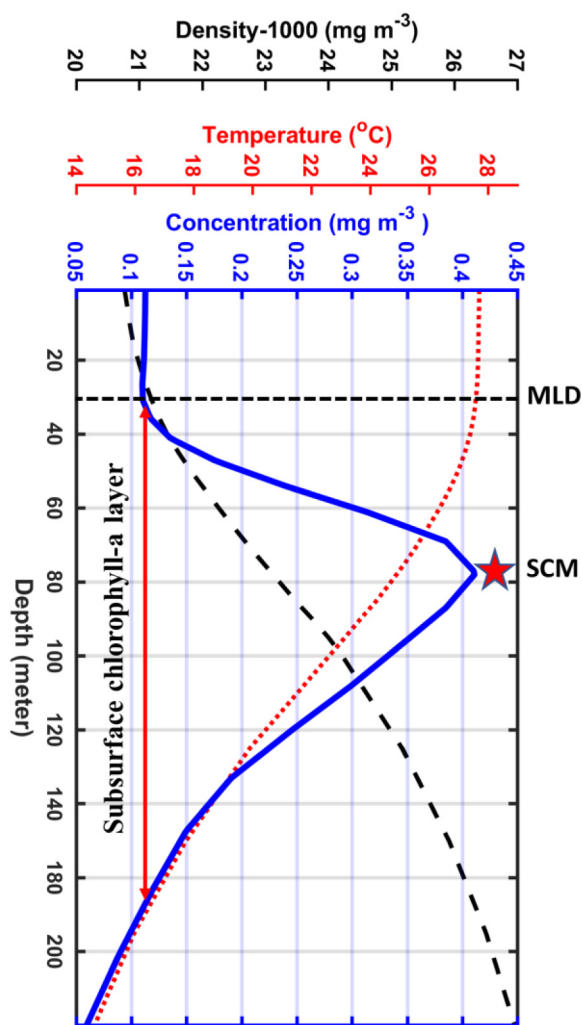


Fig. 1. Typical vertical profile of chlorophyll-a concentration (mg m^{-3}) containing subsurface chlorophyll-a maximum (SCM), temperature ($^{\circ}\text{C}$), and density (kg m^{-3}) in the Bay of Bengal. (For interpretation of the references to color in this figure legend, the reader is referred to the web version of this article.)

2019). Although remote sensing technology makes it easy to measure the surface chlorophyll-a concentration (Jeffrey et al., 1997; Picado et al., 2014), knowledge of subsurface chlorophyll-a is generally limited due to the lack of easily retrievable and readily available subsurface datasets (Brown et al., 2015; Baldry et al., 2020). Similarly, our knowledge of the subsurface chlorophyll-a distribution in the Bay of Bengal is very limited (Narvekar and Kumar, 2014; Thushara et al., 2019; Masud-Ul-Alam et al., 2020). Therefore, this study investigates the seasonal variations in the concentration and depth of the SCM to better understand the basin-wide variations in subsurface chlorophyll-a throughout the Bay of Bengal.

Generally, the conditions necessary for the chlorophyll-a concentration to increase are controlled by certain environmental physicochemical parameters such as nutrients (e.g., NO_3^- and PO_4^{3-}), water temperature, and light (Sathyendranath et al., 1991; Lewis et al., 2000; Li et al., 2017). Thus, the driving forces that affect the nutrient supply, light availability, and temperature in the water body also influence the chlorophyll-a concentration in the oceans (e.g., McCreary et al., 1996; Vinayachandran, 2005; Falkowski and Oliver, 2007; Wang et al., 2010; Narvekar and Kumar, 2014). The Bay of Bengal, which forms part of the northern Indian Ocean, is well known as a biologically less productive

zone than the adjacent latitudinally similar Arabian Sea (Radhakrishna et al., 1978; Gomes et al., 2000; Madhupratap et al., 2003; Chowdhury et al., 2017), even though the economy of the surrounding regions strongly depends on fishing activity within the Bay of Bengal (Hasan et al., 2018). Thus, the three physicochemical parameters discussed above and their driving forces are not well understood and need to be re-evaluated. Furthermore, studying these parameters can help understand the causes of low productivity in the Bay of Bengal and identify unexplored zones for fisheries.

An increase in the strength of the thermal stratification of the upper ocean water column decreases the mixing between surface and subsurface waters and diminishes the surface chlorophyll-a concentration (Wolken et al., 1955; Morel and Antoine, 1994; Bricaud et al., 2002; Zhang et al., 2016; Chowdhury et al., 2019; Trombetta et al., 2019). In the western Bay of Bengal, the sea surface temperature (SST) and surface chlorophyll-a concentration exhibit an inverse relationship. For instance, in spring, high SST-induced stratification shallows the mixed layer depth (MLD, i.e., the bottom of the mixed layer) and thus reduces the surface chlorophyll-a concentration (Madhupratap et al., 1996; Kumar et al., 2007), whereas winter cooling favors an increase in surface chlorophyll-a (Sarangi et al., 2008). Nevertheless, the role of temperature in determining the subsurface chlorophyll-a concentration in the Bay of Bengal remains unclear.

The Ganges-Brahmaputra-Meghna (GBM) River system located in the northern Bay of Bengal supplies a large amount of nutrient-rich freshwater and highly influences the chlorophyll-a concentration in summer (Kumar et al., 2002; Sengupta et al., 2006; Baliarsingh et al., 2015). However, extensive freshwater inputs can induce haline stratification (Patra et al., 2007; Chowdhury et al., 2017; Bhushan et al., 2018) and impede the transfer of nutrients to the euphotic zone from below (Gomes et al., 2000). Furthermore, during summer, suspended solids from rivers trigger high turbidity levels (Syvitski et al., 2005), ultimately reducing the penetration of light into the subsurface (Kumar et al., 2004; Bhushan et al., 2018). In addition, suspended phytoplankton may cause the water column to become more turbid. Although some studies reported that nutritious freshwater inputs from the GBM River system increase the surface chlorophyll-a concentration (e.g., Kumar et al., 2004; Li et al., 2012b; Narvekar and Kumar, 2014), contributions from the Krishna-Godavari river system and the Irrawaddy River (see Fig. 2 for the locations of these rivers) to the chlorophyll-a concentration in the Bay of Bengal have not been thoroughly explored. Moreover, the influences of stratification and turbidity on the basin-wide chlorophyll-a concentration at the SCM are not well understood and thus are investigated in this study.

The seasonally reversing monsoonal wind system in the Bay of Bengal (Shankar et al., 1996; Narvekar and Kumar, 2006; Akhter et al., 2021) may have significant effects on the chlorophyll-a concentration in this region. Southwesterly winds transport nutrient-rich, highly saline water into the Bay of Bengal from the Arabian Sea in summer (Kumar and Prasad, 1999; Vinayachandran et al., 1999). These southwesterly winds also induce coastal upwelling (Shetye et al., 1991; Muraleedharan et al., 2007; Thushara and Vinayachandran, 2016) and upward Ekman pumping along the western coast of this bay (Vinayachandran, 2004). The cold-core eddy in this bay forms throughout this year (Nuncio and Kumar, 2012, 2013; Huang et al., 2020) but becomes stronger in summer, resulting in a considerably shallower SCM (Kumar et al., 2004). These internal dynamics of the Bay of Bengal, for example, cold-core eddies and coastal upwelling, cause the thermocline layer in the Sri Lanka dome to uplift (Thushara et al., 2019). Although the existence of such internal dynamics (upwelling, eddies, and Ekman pumping) has been documented by several local studies

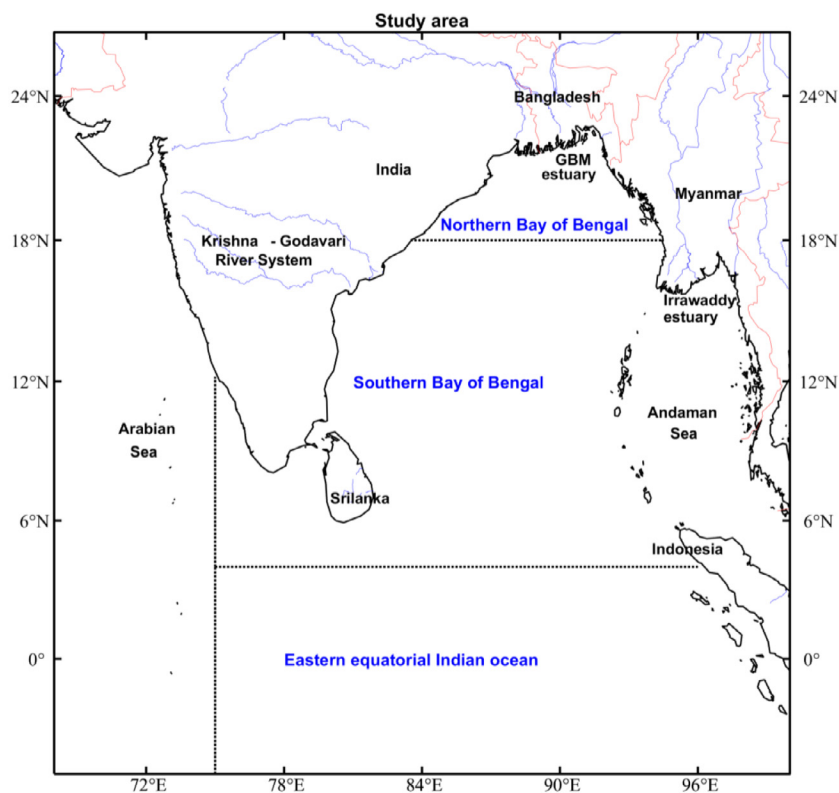


Fig. 2. The Bay of Bengal and surrounding regions (coastline, rivers, and country boundaries are indicated by black, blue, and red lines respectively). Black dot lines demarcate three sub-regions. (For interpretation of the references to color in this figure legend, the reader is referred to the web version of this article.)

(Shetye et al., 1993; Kumar et al., 2004; Muraleedharan et al., 2007; Thushara and Vinayachandran, 2016; Huang et al., 2020, a basin-wide understanding of the chlorophyll-a concentration in the water column of the Bay of Bengal due to these internal dynamics is lacking; hence, this study seeks to explore this issue.

Several investigations on the surface and/or subsurface chlorophyll-a concentration in the Bay of Bengal have focused on river inputs, the availability of sunlight, the SST, and coastal upwelling as drivers of the chlorophyll-a concentration (e.g., Gomes et al., 2000; Murty and McMurtrie, 2000; Madhupratap et al., 2003; Madhu et al., 2006; Kumar et al., 2009; Li et al., 2012b; Narvekar and Kumar, 2014; Thushara et al., 2019), but most of these studies covered only portions of the bay over short time scales. Accordingly, a higher-resolution comprehensive framework of the processes governing the surface and/or subsurface chlorophyll-a distributions and their relative effects is needed, and therefore, the following three questions are addressed in this paper.

- (1) Do major external factors (riverine nutrients, freshwater inputs, the intrusion of water from the Arabian Sea, and wind stress) and internal processes (thermocline dynamics, Ekman pumping, the MLD, and the euphotic depth) have similar effects on both the surface chlorophyll-a concentration and the SCM? If not, what are their relative contributions?
- (2) What is the primary physical forcing that triggers a thermocline shift, which can result in a change in the chlorophyll-a concentration at the SCM?
- (3) Does the depth of the SCM correlate with the depth of the thermocline?

2. Materials and method

2.1. Study area

This study focuses primarily on the Bay of Bengal, which is a part of the northern Indian Ocean (Fig. 2). To explore the equatorial influences inside the Bay of Bengal, the eastern equatorial Indian Ocean is also included in this study because it is an adjacent region that connects this bay to the equator, and fluxes are exchanged between these bodies of water. Hence, for the convenience of the systematic analyses and discussion presented herein, the study area is divided into three subregions as follows according to the different features of the chlorophyll-a distribution caused by variations in river inputs and wind forcing in the bay (Li et al., 2012b; Narvekar and Kumar, 2014; Thushara et al., 2019):

1. Northern Bay of Bengal (latitudinal range from 18°N to 23°N)
2. Southern Bay of Bengal (from 4°N to 18°N)
3. Eastern equatorial Indian Ocean (from 5°S to 4°N).

2.2. Data sources

Chlorophyll-a, nitrate (NO_3^-), phosphate (PO_4^{3-}), temperature, salinity, wind stress, and diffuse attenuation coefficient data are collected from various available data sources, which are described in the following subsections. All the data utilized in this study are collected for the same time interval (2005 to 2017). Notably, observational datasets, especially the vertical profiles of chlorophyll-a, NO_3^- , and PO_4^{3-} , are very limited in the Bay of Bengal (Narvekar and Kumar, 2014; Akhil et al., 2014; Masud-UI-Alam et al., 2020). Thus, to study the vertical structure of chlorophyll-a and its associated forcing, suitable reanalysis or

model datasets could be a better option in this region. Recently, the Copernicus Marine Environment Monitoring Service (CMEMS) has provided comprehensive datasets derived from different in situ, satellite, reanalysis, and model-based data that have been widely used in scientific studies (<https://marine.copernicus.eu/>). Therefore, we utilize chlorophyll-a, nutrients, diffuse attenuation coefficient, and surface current data from CMEMS sources.

2.2.1. Chlorophyll-a and nutrients

The global-reanalysis-bio-001-029-monthly datasets from the Pelagic Interactions Scheme for Carbon and Ecosystem Studies (PISCES) numerical model (Aumont et al., 2015) distributed by CMEMS (Noel, 2012) (<http://marine.copernicus.eu/services-portfolio/accessto-products/>) are employed as the sources of chlorophyll-a (mg m^{-3}), NO_3^- (mmol m^{-3}), and PO_4^{3-} (mmol m^{-3}) data. The horizontal resolution is $0.25^\circ \times 0.25^\circ$, and the model includes 75 layers vertically.

This PISCES model is forced offline by daily fields from an ocean dynamical simulation and from the ERA-Interim global atmospheric reanalysis datasets. The simulation is initialized with the World Ocean Atlas 2013 for nitrate, phosphate, oxygen and silicate (Garcia et al., 2014).

The model is compared with a multisensor gridded Level-3 product (OCEANCOLOUR_GLO_CHL_L3_REP_OBSERVATIONS_009_085) for a quality check (<https://catalogue.marine.copernicus.eu/documents/QUID/CMEMS-GLO-QUID-001-029.pdf>). At the sea surface, the modeled chlorophyll-a field shows good agreement (with a root mean square difference (RMSD) of 0.371 for 1997–2017) with the satellite data. In the Indian Ocean, the modeled chlorophyll-a level has a slightly negative bias (-0.182). Nevertheless, the model can reproduce the summer bloom along Somalia and the Arabian Peninsula in the Indian Ocean (Lévy et al., 2007; Koné et al., 2009) and succeeds well in reproducing the seasonal cycle at mid- and high-latitudes. The modeled nutrient concentrations (NO_3^- and PO_4^{3-}) also display good agreement with the WOA climatology at the global scale except in the Southern Ocean, where the concentrations of nutrients are too high. However, the concentrations of NO_3^- and PO_4^{3-} in the Indian and South Pacific Oceans are slightly low, although they may be increased with more precise terrestrial inputs.

2.2.2. Temperature and salinity

The monthly temperature ($^\circ\text{C}$) (Locarnini et al., 2019) and salinity (Zweng et al., 2019) climatology data are obtained from the World Ocean Atlas 2018. The horizontal resolution is $0.25^\circ \times 0.25^\circ$, and 102 layers are defined from the surface to a depth of 5,500 m. World Ocean Atlas 2018 is a collection of the available observational data, including Argo profiles, which are objectively analyzed and quality controlled (<https://www.nodc.noaa.gov/>) for analyzing data, instituting boundary and/or initial conditions in numerical models, and validating satellite data.

2.2.3. Diffuse attenuation coefficient and surface current

Data of the spectral diffuse attenuation coefficient at a wavelength of 490 nm (m^{-1}), named KD (490), are derived from satellite-based monthly products merged from SeaWiFS, MODIS, MERIS, VIIRS-SNPP&JPSS1, and OLCI-S3 A&S3B data using the Morel algorithm (Doron et al., 2006; Morel et al., 2007). KD (490) demonstrates a good correlation (R^2 of 0.8) and small RMSD (0.21) with observations, and the grid resolution is 4 km.

The monthly surface current data (zonal and meridional velocities) used in this study are derived from MULTIOBS, a satellite-derived gridded product (Bonjean and Lagerlorf, 2002; Copernicus Marine In Situ Tac, 2020). This product utilizes a methodology similar to the popular Ocean Surface Current Analyses Real-time (OSCAR) system data and gives good results when compared

with the OSCAR data. Coastal biases are removed in MULTIOBS, but some biases remain in the tropics and western boundary currents. The RMSDs of the zonal velocity (0.146) and the meridional velocity (0.147) are the same compared with the observations (Argo float-derived velocities). The horizontal resolution is $0.25^\circ \times 0.25^\circ$.

2.2.4. Wind speed and wind stress curl

The monthly mean zonal and meridional components of the wind velocity (m s^{-1}) at 10 m above the ground used in this study are taken from the widely used ERA-Interim dataset produced by the European Centre for Medium-range Weather Forecast (ECMWF) (2011). The wind stress curl (N m^{-3}) is then calculated from the wind velocity with a grid resolution of 0.25° .

2.3. Methods

2.3.1. Data processing

The current study attempts to analyze the monthly/seasonal cycles of each variable. The temperature and salinity data are directly downloaded as their monthly mean climatologies (12 months). In contrast, the chlorophyll-a, NO_3^- , PO_4^{3-} , wind stress, surface current, and diffuse attenuation coefficient data are downloaded as monthly means over 13 years of data (2005–2017) and are then converted into their monthly mean climatologies (12 months) by a simple averaging method. In this study, the seasons are considered as follows according to Thadathil et al. (2007) and Shee et al. (2019): winter (December to February), spring (March to May), summer (June to September) and autumn (October to November). Although the temporal resolution is the same (2005–2017) among all the datasets extracted from different sources, the spatial resolutions among some of these datasets are uneven, and thus, the data are linearly interpolated to a common spatial grid. Likewise, the vertical resolutions of some datasets are also unequal, and thus, the data are linearly interpolated with a 1-m depth interval to improve the comparability among the variables.

2.3.2. Calculation of different parameters

The depth of the SCM in this study is defined as an increase in the chlorophyll-a concentration in the water column by at least 0.05 mg m^{-3} relative to the surface concentration (Fig. 1). The euphotic depth (m) is the depth where the light field decreases to 1% of the light at the surface and is calculated based on KD (490) after Kirk (1994) as euphotic depth = $4.6/\text{KD}$ (490). Since KD (490) can reflect the turbidity in the water, it is also regarded as a proxy of turbidity (m^{-1}) in the rest of this paper.

The water density calculated from the temperature and salinity gridded data collected from the WOA climatology is used to calculate the MLD. In this study, an increase of 0.2 kg m^{-3} in the surface density is used as the fixed-density criterion to determine the MLD (Monterey and Levitus, 1997; Girishkumar et al., 2013; Thadathil et al., 2002, 2016). The depth of the 26°C isotherm is considered a proxy of the thermocline depth in the current study.

The Brunt–Väisälä frequency is calculated from the water density following equation (Roseli et al., 2015):

$$N^2 = -\frac{g}{\rho} \frac{\Delta\rho}{\Delta z}$$

where N = Brunt–Väisälä frequency, g = gravitational acceleration, ρ = potential density, $\Delta\rho$ = difference between the potential densities of two water parcels, and Δz = the vertical distance between the two water parcels. If $N^2 > 0$, the stratification is stable, and overturning does not occur locally.

2.3.3. Empirical orthogonal function (EOF) and statistical analyses

The EOF method has been widely discussed by different authors (e.g., De Viron et al., 2006; Rangelova, 2007; Kusche et al., 2011) as well as in textbooks (e.g., Preisendorfer and Mobley, 1988; Jolliffe et al., 2003) and is utilized to analyze the spatial and temporal variability of geophysical data (Bjornsson and Venegas, 1997). The time series of a variable can be decomposed by $\sum_{i=1}^N PC(t_i) \cdot EOF(x_i, y_i)$, where $EOF(x_i, y_i)$ represents the spatial structures of the major factors and $PC(t)$ denotes the principal components that state how the amplitude of each EOF mode varies with time. The first EOF mode is responsible for the largest component of the variance, followed by the second mode, etc.

The aim of the current investigation is to reveal the spatial and temporal relationships of the monthly mean concentration of chlorophyll-a at both the surface and the SCM with its causative parameters (wind stress curl, MLD, depth of the 26 °C isotherm, temperature, salinity, turbidity and nutrients). For this purpose, all relevant (multiple) variables are systematically employed in a single-variable EOF analysis (Preisendorfer and Mobley, 1988; Enfield and Mestas-Nuñez, 1999), known as multivariate EOF decomposition. More specifically, chlorophyll-a and all other physical control variables are combined into a large data matrix (all variables are standardized), and then EOF decomposition is performed. The size of the data matrix is $cm * n$ (multiple) instead of $m * n$ (single), in which 'c' is the number of variables, 'm' is the number of pixels in the spatial region for each variable, and 'n = 12 months' is the number of times. The data are arranged in sequence variable by variable, so the eigenvector obtained for each EOF mode is equally divided into 'c' segments, with each segment corresponding to a spatial pattern for one variable. In addition, the principal component (PC) for each (multivariate) EOF mode contains only one common time series. The advantage of this method is that the relationships among all (physical) variables (as well as the relationship between any two pixels) are considered. Notably, a strongly coupled zone of variance among relevant variables for the same period is identified from the multivariate EOF decomposition, and then this EOF pattern is interpreted in terms of potential regional physical processes to establish a significant relationship among multiple variables. In this study, the spatial EOF modes are denoted EOF1, EOF2, and EOF3 (in ascending order of dominant modes), and their corresponding temporal modes are denoted PC1, PC2, and PC3, respectively.

In addition, another method is used to study the relationships between chlorophyll-a and the other physical control variables. The correlation fields between PC1 (the first dominant mode) derived from the single-variable EOF decomposition of the surface chlorophyll-a concentration and the 3D dataset of each physical control variable (e.g., MLD, salinity) are determined; these fields are known as heterogeneous correlation maps (Bjornsson and Venegas, 1997). These spatiotemporal correlations are determined between the response and control variables with a significance level greater than 95% in the current study. Finally, the gridded mean correlations between the chlorophyll-a concentration at both the surface and the SCM and its probable control parameters are determined for selected potential zones.

3. Results

The spatial and temporal variations of the chlorophyll-a concentrations at both the surface and the SCM depend primarily on river inputs, the influences from adjacent seas, the available nutrient supply, and the regional wind dynamics. Hence, the distributions of the chlorophyll-a concentration at both the surface and the SCM are evaluated comprehensively along with their control mechanisms in the northern Bay of Bengal, southern Bay of Bengal, and eastern equatorial Indian Ocean in the following subsections.

3.1. Seasonal distributions of chlorophyll-a at the surface and the SCM

The chlorophyll-a concentrations at the surface and the SCM and the depth of the SCM differ both seasonally and spatially in the Bay of Bengal and the eastern equatorial Indian Ocean (Figs. 3–4).

3.1.1. Northern Bay of Bengal

In the northern Bay of Bengal, the surface chlorophyll-a concentration is the highest (0.3 to 4 mg m⁻³) during summer but slightly reduces in autumn, decreases further in winter, and becomes the lowest (0.1 to 1 mg m⁻³) in spring (first row in Fig. 3). During summer and autumn, high surface chlorophyll-a concentrations (0.2 to 4 mg m⁻³) cover the entire northern part of the bay and are observed along the western coast and slightly toward the eastern coast of the bay (Figs. 3c1–d1). During winter and spring, high chlorophyll-a concentrations are confined to the mouth of the GBM River estuary; however, a band of high chlorophyll-a concentrations (0.2 to 1 mg m⁻³) also extends to the eastern coast of the bay during winter (Figs. 3a1–b1).

The seasonal variations in the chlorophyll-a concentration at the SCM are subtle in the northern Bay of Bengal, as the SCM remains high (0.8 to 2 mg m⁻³) throughout the year along the coastal belt (first row in Fig. 4). Furthermore, the depth of the SCM remains shallow (20 to 45 m) along the coastal belt but occurs at deeper depths (45 to 70 m) in the offshore regions of the bay throughout the year (second row in Fig. 4).

3.1.2. Southern Bay of Bengal

During summer, three zones of high surface chlorophyll-a concentrations (0.2 to 2 mg m⁻³) are observed in the southern Bay of Bengal: along the western coast near the Krishna–Godavari River system, at the mouth of the Irrawaddy River, and within the Sri Lanka dome (Fig. 3c1; see Fig. 1 for locations). During autumn, a similar spatial distribution of surface chlorophyll-a is observed, but the chlorophyll-a concentration is slightly reduced compared with that in summer. During winter, a band of high surface chlorophyll-a concentrations (0.1 to 0.2 mg m⁻³) is discernible only along the western coast (Fig. 3a1). In spring, the surface chlorophyll-a concentration is the lowest (0.05 to 0.1 mg m⁻³) throughout the bay (Fig. 3b1). Overall, throughout the year, the surface chlorophyll-a concentration is higher along the coastline and the western coast than in the rest of the bay (first row in Fig. 3).

During summer, the chlorophyll-a concentration at the SCM is significantly higher (0.4 to 0.6 mg m⁻³) along the western side of the southern Bay of Bengal (including the Sri Lanka dome) than during the other seasons (Fig. 4c1). The observed high SCM concentrations occur at shallow depths (45 to 65 m). A similar spatial distribution of the SCM is observed during autumn, albeit with lower chlorophyll concentrations and deeper SCMs than in summer. In addition, the chlorophyll-a concentration at the SCM in winter is lower than that during the other seasons. Notably, during spring, high chlorophyll-a concentrations (ranging from 0.4 to 0.5 mg m⁻³) are observed at the SCM throughout the southern Bay of Bengal (Fig. 4b1), although the surface chlorophyll concentration is the lowest; moreover, the SCM occurs at the deepest depth (~90 m) during the spring. In general, the chlorophyll-a concentration at the SCM is higher and the SCM depth is shallower in the west than in the east (second row in Fig. 4). Additionally, along the mouth of the Irrawaddy River, the chlorophyll-a concentration at the SCM remains high throughout the year (0.6 to 1 mg m⁻³), and the SCM occurs at relatively shallow depths (20 to 50 m) (Figs. 4a1–d1).

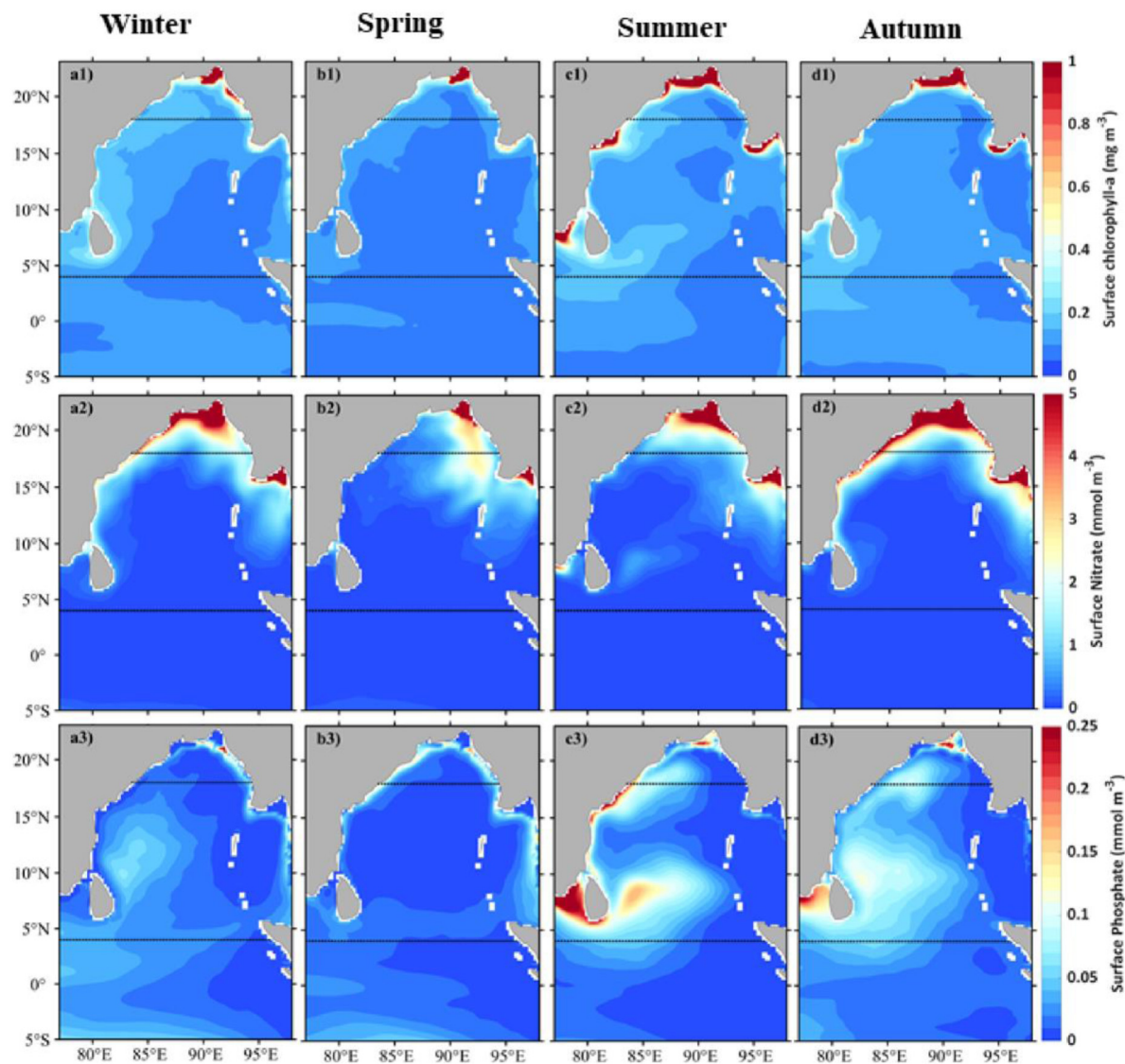


Fig. 3. Seasonal variation of surface chlorophyll-a concentration (mg m^{-3}) (first row), NO_3^- (mmol m^{-3}) (second row), and PO_4^{3-} (mmol m^{-3}) (third row). Black dot lines demarcate three sub-regions. (For interpretation of the references to color in this figure legend, the reader is referred to the web version of this article.)

3.1.3. Eastern Equatorial Indian Ocean

The surface chlorophyll-a concentration ranges from 0.05 to 0.1 mg m^{-3} in the eastern equatorial Indian Ocean and remains low throughout year compared to the Bay of Bengal (first row in Fig. 3). In addition, the surface chlorophyll-a concentration remains slightly high during autumn and winter ($\sim 0.1 \text{ mg m}^{-3}$) and reaches a minimum ($\sim 0.05 \text{ mg m}^{-3}$) in spring. Similar to that at the surface, the concentration of chlorophyll-a at the SCM is lower in this equatorial region throughout year, and the depth of the SCM (60 to 90 m) is substantially deeper than that in other parts of the study area (Fig. 4).

3.2. Driving mechanisms of the spatial, temporal, and vertical distributions of chlorophyll-a

Typically, the forcing factors of the vertical distribution of chlorophyll-a (i.e., at both the surface and the SCM) within a given region should be similar, as they can be affected by identical hydrological and oceanic mechanisms. Thus, multivariate EOF analyses are performed separately for the chlorophyll-a concentrations both at the surface (Fig. 5) and at the SCM (Fig. 6) with their respective responsible variables (e.g., salinity, turbidity,

NO_3^- , PO_4^{3-} , depth of 26° isotherm, wind stress curl). Furthermore, two-dimensional correlation coefficient maps between the time series (PC1) of surface chlorophyll-a and the grid cells of the three-dimensional spatiotemporal datasets of the individual control variables (sea surface salinity (SSS), turbidity, NO_3^- , PO_4^{3-} , SST, and MLD) are calculated to establish the spatial relationships between them (Fig. 7). The dominant mode of the single-variable (surface chlorophyll-a concentration) EOF decomposition accounts for approximately 95% of the total variance, showing substantially positive variability in five potential zones during the second half of the year (Figs. 7a–b). Furthermore, the correlations between the chlorophyll-a concentrations and their associated forcing variables in the selected potential zones are listed for the chlorophyll-a concentrations at both the surface (Table 1) and the SCM (Table 2).

3.2.1. Northern Bay of Bengal

The dominant mode obtained from the multivariate EOF decomposition of the chlorophyll-a concentrations at both the surface and the SCM and their possible driving factors show strong seasonal variations (Figs. 5 and 6). The combination of EOF1 and PC1 of the chlorophyll-a concentration at both the surface and

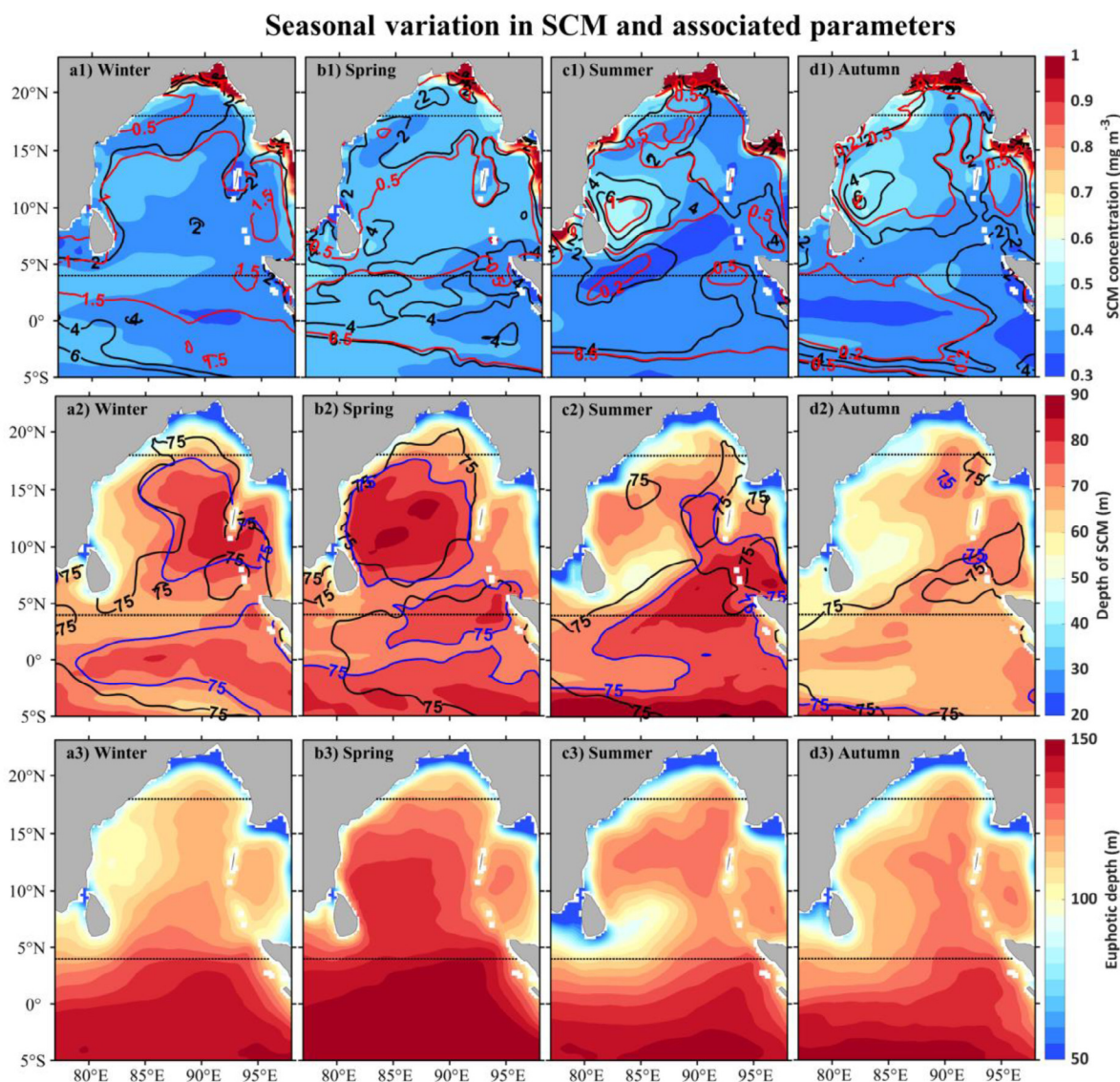


Fig. 4. Seasonal distribution of the SCM (mg m^{-3}) (shading), NO_3^- (mmol m^{-3}) (black contour) and PO_4^{3-} (mmol m^{-3}) (red contour) at the same depth (first row); the depth (m) of the SCM overlaid with its contour (75 m) (blue color) and contour of the depth (m) of 26 °C isotherm (black color) (second row); and euphotic depth (m) (third row). Black dot lines demarcate three sub-regions. (For interpretation of the references to color in this figure legend, the reader is referred to the web version of this article.)

the SCM exhibits positive variability during summer and early autumn along the northern and western coasts of the northern Bay of Bengal (Figs. 5a–b and 6a–b). This positive variation corresponds to the observed high chlorophyll-a concentration at the surface and SCM during these seasons (described in Section 3.1.1).

During summer and early autumn, SSS displays strong negative variability along the northern coastline (Fig. 5c). The presence of low-salinity water is also evident from the spatial distribution of SSS (30 to 31) (Figs. 8c–d). The salinity at the SCM also exhibits negative variability during these seasons (Fig. 6c). A large amount of freshwater from the GBM River system and monsoonal precipitation are the sources of low-salinity water in this bay (Webster, 1987; Fluteau et al., 1999; Akhil et al., 2014). This nutritious riverine low-salinity water is significantly correlated with the high surface chlorophyll-a concentration during these seasons ($r = -0.51$, p -value = 0.04, Table 1 and Figs. 3, 7c). The significant correlation between the surface chlorophyll-a concentration and turbidity ($r = 0.63$) (Table 2) evidences the presence of suspended phytoplankton and nutrient-rich turbid riverine water. The haline stratification generated by this

low-salinity water (Fig. 9) causes the MLD to be shallow in the northern Bay of Bengal (Gopalakrishna et al., 2002; Akhil et al., 2014), and this shallow MLD is negatively correlated with the surface chlorophyll-a concentration in this part of the bay (Fig. 7e) and helps uplift the thermocline (26 °C isotherm) during summer and early autumn (Figs. 5e–f). A positive wind stress curl (upward Ekman pumping) also helps uplift the thermocline during these seasons (Fig. 5g), and Ekman pumping enhances the surface chlorophyll-a concentration ($r = 0.64$, p -value = 0.01, Table 2). The inverse correlation ($r = -0.69$) between the chlorophyll-a concentration at the SCM and the thermocline depth indicates that a shallow thermocline might also enhance the chlorophyll-a concentration at the SCM (first row in Fig. 4). In addition, the shallow thermocline is spatially correlated to the depth of the SCM, as both are uplifted in the northern part of the bay (second row in Fig. 4). Although the nutrients (NO_3^- and PO_4^{3-}) transported by continental rivers show positive variability in the multivariate EOFs (Figs. 5h–i), the spatial relationship between the surface chlorophyll-a and NO_3^- ($r = 0.61$, p -value =

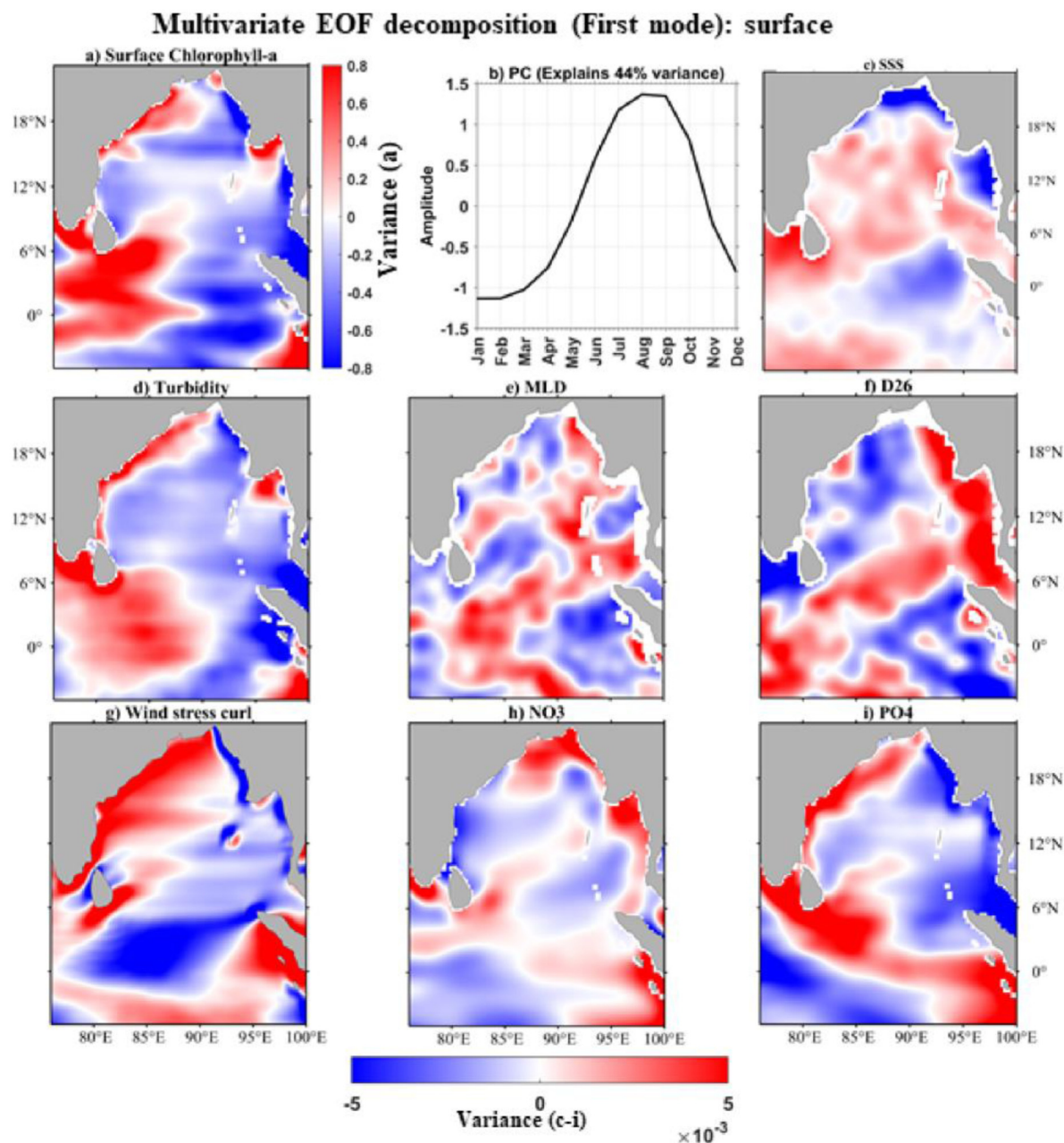


Fig. 5. Multivariate EOF decomposition (EOF1, first dominant mode) of surface chlorophyll-a (mg m^{-3}) (a), common PC for all variables (b), SSS (c), turbidity (m^{-1}) (d), MLD (m) (e), depth of 26 °C isotherm (f), wind stress curl (N m^{-3}) (g), (NO_3^-) (mmol m^{-3}) (h), and (PO_4^{3-}) (mmol m^{-3}) (i). (For interpretation of the references to color in this figure legend, the reader is referred to the web version of this article.)

0.03) is slightly weaker than the relationship between the surface chlorophyll-a and PO_4^{3-} ($r = 0.8$, p -value = 0.00) (Table 1, Fig. 3). However, NO_3^- is more correlated with the concentration of chlorophyll-a at the SCM than is PO_4^{3-} (Table 2). Primary production may be nitrogen-limited in this area (Kumar et al., 2002). Therefore, nutritious freshwater from the GBM River system keeps the concentration of chlorophyll-a high at both the surface and the SCM, and this strong freshwater-induced stratification is responsible for shoaling of the SCM during summer and early autumn in the northern Bay of Bengal.

During winter and spring, the concentration of chlorophyll-a both at the surface and at the SCM exhibits discernible negative variability (Figs. 5a–b, 6a–b), which corresponds to the observed distribution of low chlorophyll-a concentrations described in Section 3.1.1. The variations in the probable driving forces also correspond to the low chlorophyll-a concentrations

during these seasons (Figs. 5–6). For instance, the dominant EOF mode shows positive variability in the SSS and salinity at the SCM during these seasons. Drastic reductions in river discharge and precipitation keep the SSS higher during winter and spring than during summer and autumn (Narvekar and Kumar, 2014; Bhushan et al., 2018). Comparatively high-salinity water in conjunction with a negative wind stress curl-induced deep thermocline (Figs. 5f–g, 6d–e) cannot sufficiently increase the supply of nutrients in the upper ocean, resulting in the reduced concentration of chlorophyll-a at both the surface and the SCM during these seasons. The deep thermocline during winter and spring deepens the depth of the SCM (second row in Fig. 4) and further reduces the concentration of chlorophyll-a at the SCM during these seasons. On the other hand, a band of high chlorophyll-a at both the surface and the SCM along the eastern coast during winter is observed due to the positive wind stress

Multivariate EOF decomposition (First mode): SCM

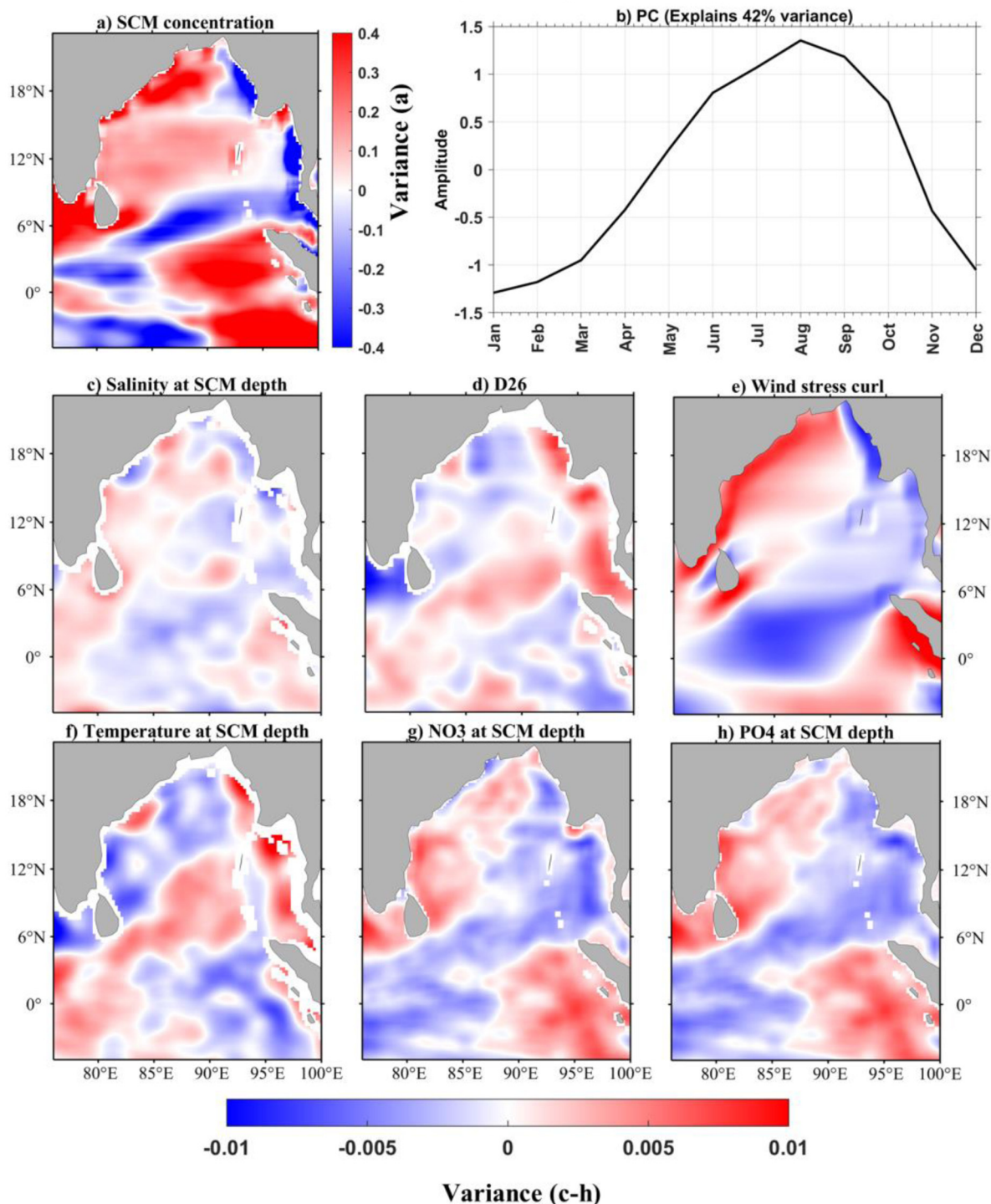


Fig. 6. Multivariate EOF decomposition (EOF1, first dominant mode) of concentration of chlorophyll-a at SCM (mg m^{-3}) (a), common PC for all variables (b), Salinity at the depth of SCM (c), turbidity (m^{-1}) (d), MLD in meter (e), depth of 26 °C isotherm (f), wind stress curl (Nm^{-3}) (g), NO_3^- at the depth of SCM (mmol m^{-3}) (h), and PO_4^{3-} at the depth of SCM (mmol m^{-3}) (i). (For interpretation of the references to color in this figure legend, the reader is referred to the web version of this article.)

curl-induced shallow thermocline along this band (Figs. 5g, 6e). Notably, northeasterly winds favor upwelling along the eastern coast in winter (Suryanarayana et al., 1993; He et al., 2020). Therefore, the reduced freshwater input and negative wind stress curl are responsible for the low chlorophyll-a concentrations at

both the surface and the SCM during winter and spring in the northern Bay of Bengal.

3.2.2. Southern Bay of Bengal

The dominant modes of both the multivariate EOF analysis (Figs. 5a–b) and the single-variable EOF analysis (Figs. 7a–b) exhibit positive variability in the surface chlorophyll-a near the

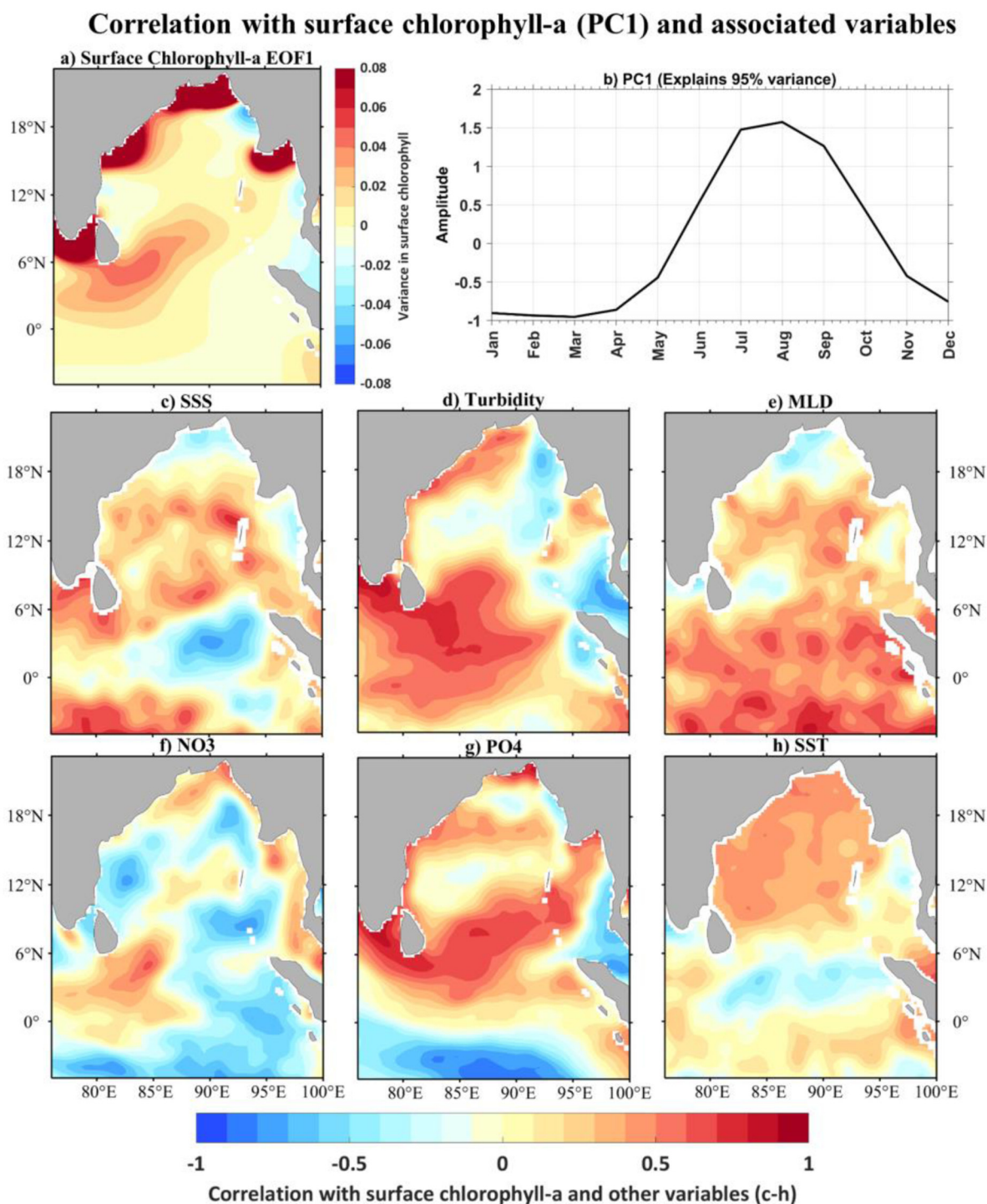


Fig. 7. EOF1 (a) and PC1 (b) of surface chlorophyll-a concentration. Correlation coefficient between PC1 of surface chlorophyll-a with SSS (c), turbidity (d), MLD (e), NO_3^- (f), PO_4^{3-} (g), and SST (h). (For interpretation of the references to color in this figure legend, the reader is referred to the web version of this article.)

Irrawaddy River estuary in the east, the Krishna–Godavari river system on the northwestern coast, and the Sri Lanka dome on the southwestern side of the southern Bay of Bengal during summer and early autumn. These three plausible zones characterized by a high surface chlorophyll-a concentration are also revealed from the spatial distribution of surface chlorophyll-a (Figs. 3c–d). The SCM also shows positive variability in these three zones (Figs. 6a–b). In addition, the chlorophyll-a concentration at the SCM is also observed to exhibit positive variability along the entire western part of the southern Bay of Bengal during summer

and early autumn (Figs. 6a–b). Furthermore, negative variability in the SSS and salinity at the SCM (Figs. 5b–c, 6b–c) and positive variability in turbidity (Fig. 5d) and nutrients (Figs. 5h–i) are found in the southern Bay of Bengal near the Irrawaddy River estuary during summer and autumn. The spatial correlations of SSS (negative), turbidity (positive), and nutrients (positive) with the surface chlorophyll-a concentration in this zone indicate that the Irrawaddy River might be the source of nutritious low-salinity water in this part of the bay (Figs. 7a–d, f–g). The presence of a

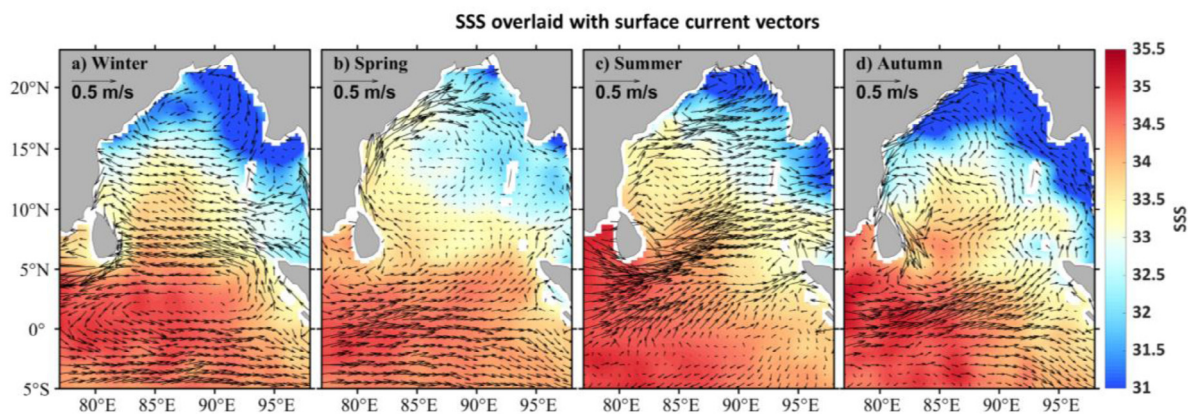


Fig. 8. Seasonal variation of SSS and surface current vectors (m s^{-1}). (For interpretation of the references to color in this figure legend, the reader is referred to the web version of this article.)

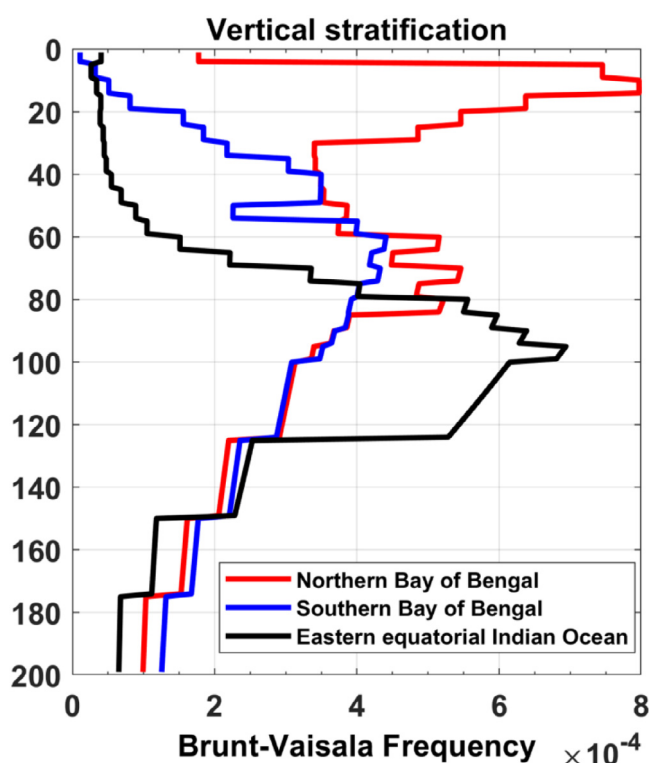


Fig. 9. Stratification profiles (averaged over all pixels and time periods) along the northern Bay of Bengal, the southern Bay of Bengal, and the eastern equatorial Indian Ocean. Fig. 2 illustrates the regions. (For interpretation of the references to color in this figure legend, the reader is referred to the web version of this article.)

high concentration of chlorophyll-*a* at the SCM in this region (hydrologically similar to a high surface chlorophyll-*a* concentration) might also be due to nutrient-rich freshwater input. However, the negative wind stress curl (negative variability) and associated deepening of the thermocline are disadvantageous to the increases in the chlorophyll-*a* concentration at both the surface and the SCM in this part of the bay (Figs. 5f–g, 6d–e). Hence, nutrient inputs from the Irrawaddy River are the main driver in increasing the chlorophyll-*a* concentrations at both the surface and the SCM in the Irrawaddy River estuary.

During summer and early autumn, salinity demonstrates positive variability in the entire western part of the southern Bay of Bengal (Figs. 5c, 6c) with comparatively higher SSS (32 to

33.5) (Figs. 8c–d). The presence of highly saline water indicates that continental river input has no control over the salinity in this region; rather, the input of saltier water from the surrounding regions or from underneath might dominate the input of river discharge. The intrusion of saline water from the highly productive Arabian Sea is evident from the spatial distributions of the surface current and SSS (Figs. 8c–d). During the summer monsoon, the Bay of Bengal is affected by a strong southwesterly wind (Shankar et al., 1996; Narvekar and Kumar, 2006), which rapidly generates upward Ekman pumping (positive variability), resulting in the upwelling of cold saltier water from underneath and the subsequent uplift of the thermocline (negative variability) throughout the entire western part of the bay (Figs. 6c–f). The SCM also occurs at relatively shallow depths in the western part of the bay during summer and autumn (second row in Fig. 4). The concentration of chlorophyll-*a* at the SCM has a significant correlation with the occurrence of upward Ekman pumping ($r = 0.51$) and the thermocline depth ($r = -0.90$) throughout the entire western part of the southern Bay of Bengal (Table 2), which is further characterized by NO_3^- and PO_4^{3-} both showing positive variability with the concentration of chlorophyll-*a* at the SCM (Figs. 6g–h), and the chlorophyll-*a* concentration at the SCM is significantly positively correlated with NO_3^- ($r = 0.57$) and PO_4^{3-} ($r = 0.51$) at the depth of the SCM (Table 2). Therefore, the uplift of the thermocline and subsequent enrichment of nutrients are the main drivers of the increased concentration of chlorophyll-*a* at the SCM throughout the whole western part of the southern Bay of Bengal during summer and early autumn.

Although a high concentration of chlorophyll-*a* at the SCM spreads throughout the entire western side of the southern Bay of Bengal, surface chlorophyll-*a* is confined to the western coastal belt and along the Sri Lanka dome (Figs. 5a, 6a) because the discussed forcing on the western side of this bay might not be sufficiently strong to enrich the surface with nutrients. The abundance of surface chlorophyll-*a* along the western coast of the southern Bay of Bengal could be explained by the prevailing direction of the zonal wind stress. The zonal wind stress is directed northeastward from the coast during summer (Vinayachandran et al., 1999; Vinayachandran, 2005), which is discernible from the direction of the surface current along the western coast (Fig. 8c). This Ekman drift-generated coastal upwelling transports nutritious saltier water from beneath, and this water, which is confined mostly along the western coast of the southern Bay of Bengal during summer and early autumn, enriches the chlorophyll-*a* concentrations at both the surface and the SCM (Figs. 3c–d, 4c1–d1). This finding is also supported by the significant correlation between the surface chlorophyll-*a* concentration and the zonal

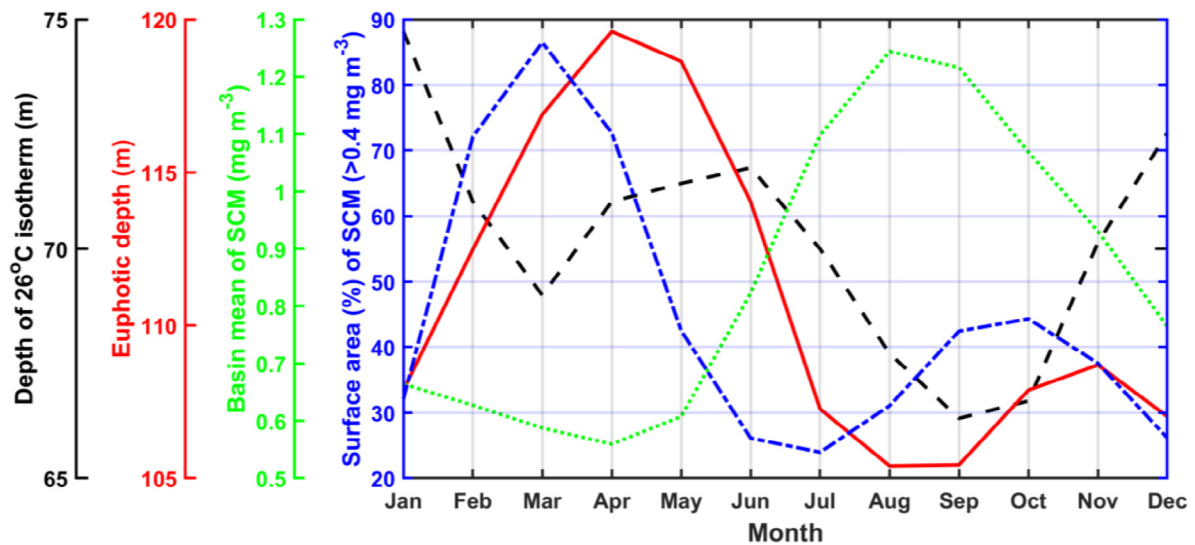


Fig. 10. Surface area (% of total study domain) covered by high concentration of chlorophyll-a location at SCM ($>0.4 \text{ mg m}^{-3}$), basin averaged monthly variation of the SCM (mg m^{-3}), euphotic depth (m), and depth (m) of 26°C isotherm. For each month, the values of each variable are averaged over the whole study region. (For interpretation of the references to color in this figure legend, the reader is referred to the web version of this article.)

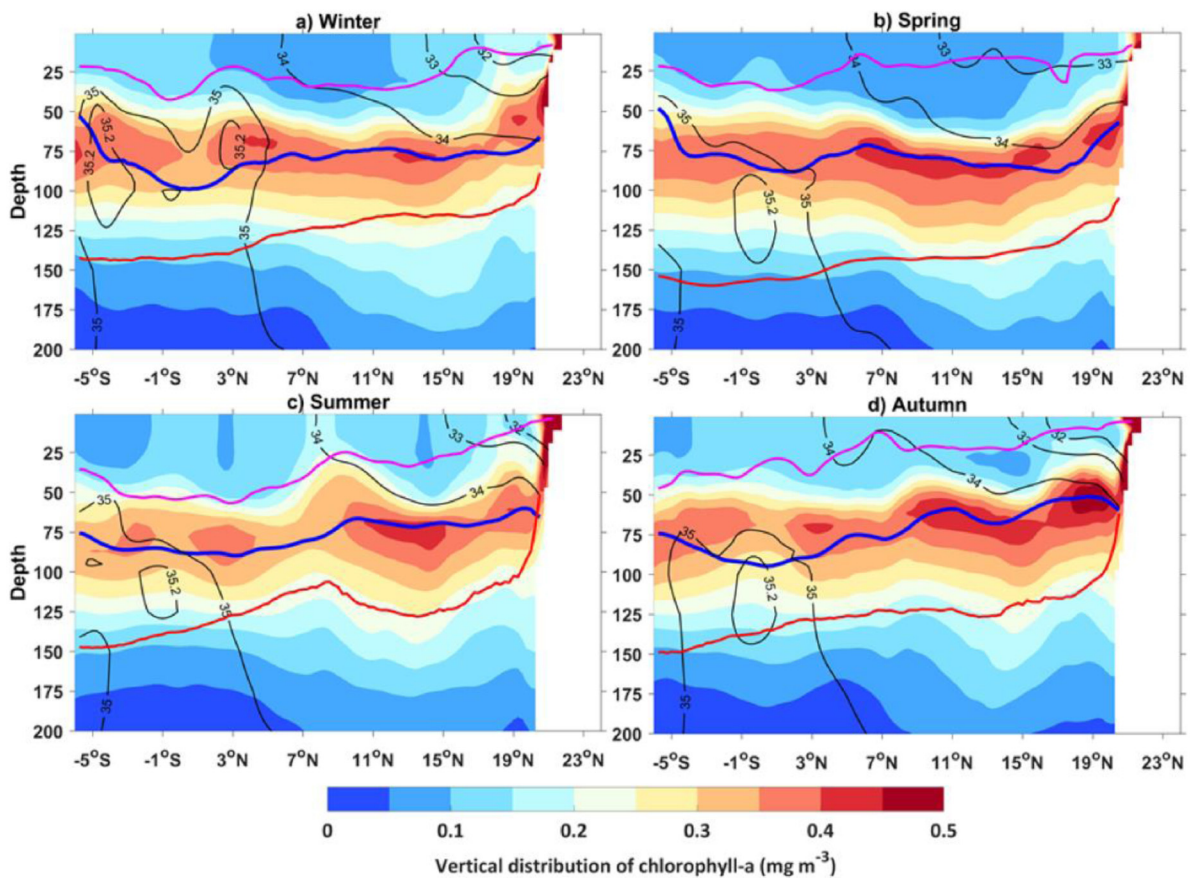


Fig. 11. Seasonal vertical distribution of the chlorophyll-a concentration (mg m^{-3}) (shading) overlaid with contours of associated variables (salinity in black, MLD (m) in magenta, depth of 26°C isotherm (m) in blue, and euphotic depth (m) in red color contours) in the north-south vertical section along the 88°E longitude. (For interpretation of the references to color in this figure legend, the reader is referred to the web version of this article.)

wind stress ($r = 0.73$) and upward Ekman pumping ($r = 0.68$) along this coastline (Table 1). Within the Sri Lanka dome, the northeastward strong surface current and intruding signature of SSS (33 to 35) also indicate the influence of saltier water from the Arabian Sea (Fig. 8c). In addition, the surface chlorophyll-a concentration shows a noteworthy correlation with the occurrence

of Ekman pumping ($r = 0.76$) and the thermocline depth ($r = -0.80$) (Table 1). Therefore, upward Ekman pumping and water from the Arabian Sea are sources of the surface and subsurface nutrients in this dome. Notably, PO_4^{3-} is more correlated than NO_3^- with the surface chlorophyll-a concentration, while both NO_3^- and PO_4^{3-} are strongly correlated with the concentration of

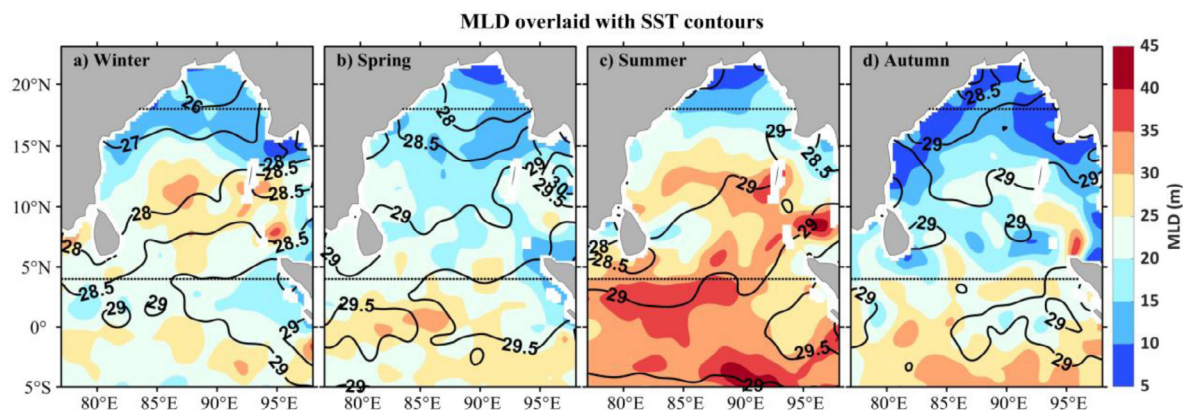


Fig. 12. Seasonal distribution of MLD (shading) and SST (contours). Black dot lines demarcate three sub-regions. (For interpretation of the references to color in this figure legend, the reader is referred to the web version of this article.)

Table 1
Correlations between surface chlorophyll-a concentration and related variables along five potential zones in surface.

Variables	Northern Bay of Bengal		Irrawaddy		Krishna–Godavari		Sri Lanka dome		Indonesia dome	
	r	p-value	r	p-value	r	p-value	r	p-value	r	p-value
SSS	<i>-0.51</i>	0.04	-0.4	0.1	0.15	0.43	<i>0.67</i>	0.02	<i>0.43</i>	0.02
Turbidity	<i>0.63</i>	0.03	<i>0.65</i>	0.02	<i>0.76</i>	0	<i>0.97</i>	0	<i>0.91</i>	0.00
Nitrate	<i>0.61</i>	0.03	0.26	0.41	-0.15	0.65	-0.24	0.46	0.59	0.07
Phosphate	<i>0.85</i>	0	<i>0.66</i>	0.02	<i>0.83</i>	0	<i>0.85</i>	0	<i>0.91</i>	0.00
MLD	-0.48	0.1	0.25	0.43	0.1	0.77	-0.2	0.12	-0.30	0.25
SST	<i>0.71</i>	0.01	0.35	0.27	<i>0.38</i>	0.22	-0.28	0.38	<i>-0.83</i>	0.00
Ek. P	<i>0.64</i>	0.01	0.18	0.58	<i>0.68</i>	0.03	<i>0.76</i>	0.02	<i>0.49</i>	0.04
D26	<i>-0.64</i>	0.02	0.52	0.08	-0.48	0.5	<i>-0.8</i>	0	-0.40	0.09
Zonal wind	0.55	0.05	<i>0.59</i>	0.04	<i>0.73</i>	0.03	<i>0.6</i>	0.04	0.40	0.20

Note: More than 95% significant correlations are Italic boldfaced. D26 stands for the depth of 26 °C isotherm, Ek. P stands for Ekman pumping, and zonal wind stands for zonal wind stress. Zones are defined as follows: northern Bay of Bengal (82 to 100°E, 18 to 23°N), Irrawaddy (92 to 98°E, 15 to 18°N), Krishna–Godavari (78 to 86°E, 15 to 18°N), Sri Lanka dome (75 to 86°E, 6 to 10°N), Indonesia dome (92 to 100°E, 5°S to 4°N).

Table 2
Correlations between chlorophyll-a concentration at SCM and associated variables along three potential zones in subsurface.

Variables	Northern Bay of Bengal		West BoB		Indonesia dome	
	r	p-value	r	p-value	r	p-value
Ekman pumping	0.45	0.10	<i>0.51</i>	0.03	0.2	0.35
D26	<i>-0.69</i>	0.01	<i>-0.90</i>	0	<i>-0.68</i>	0.03
Nitrate	<i>0.99</i>	0.00	<i>0.57</i>	0.04	0.42	0.06
Phosphate	0.40	0.20	<i>0.51</i>	0.04	<i>0.51</i>	0.04
Depth of SCM	<i>-0.64</i>	0.03	<i>-0.85</i>	0	<i>-0.52</i>	0.05
Zonal wind stress	0.51	0.05	<i>0.6</i>	0.02	<i>0.5</i>	0.04

Note: More than 95% significant correlations are Italic boldfaced. D26 stands for the depth of 26 °C isotherm. Zones are defined as follows: western Bay of Bengal (75 to 90°E, 4 to 23°N), and others are same as in Table 1.

chlorophyll-a at the SCM in the entire southern Bay of Bengal (Tables 1–2).

Along the western coast of the southern Bay of Bengal, a band of high surface chlorophyll-a concentrations is observed during winter (Fig. 3a), as was observed in a previous study (Lévy et al., 2007; Vinayachandran et al., 2013). The residual low-salinity water remaining after monsoonal precipitation and river discharge along the northern Bay of Bengal spreads out with a time lag during winter (Fig. 8a) hugging the western coast of the bay following the East India Coastal Current (Shetye et al., 1996) and eventually retains a large amount of surface chlorophyll-a along the western coast of this bay. Notably, the second multivariate EOF mode of the surface variables (e.g., nutrients and surface chlorophyll-a) also captures this phenomenon along the western boundary during autumn to early winter (figure not shown). However, the variability of surface chlorophyll-a is negative in

the remaining part of the southern Bay of Bengal. Moreover, the negative variability of the chlorophyll-a concentration at the SCM is observed in the southern Bay of Bengal during autumn to early winter (Figs. 6a–b). A negative wind stress curl-induced deep thermocline (Figs. 5g, 6d–e) might be responsible for the low concentration of chlorophyll-a in the southern Bay of Bengal at both the surface (except western boundary) and the SCM during winter.

In spring, a high SSS with low turbidity indicates the presence of less continental water and less suspended phytoplankton in the southern Bay of Bengal (Fig. 8b). Moreover, the negative variability of the wind stress curl indicates that subsurface nutrients do not have a significant contribution at the surface (Fig. 5g). During spring, a weak wind blows over this bay (Rao and Sastry, 1981; Han et al., 2010), which might maintain the negative variability of the wind stress curl. Furthermore, low surface chlorophyll-a concentrations are positively correlated with the thermally stratified shallow MLD in the southern Bay of Bengal during spring (Fig. 7). Although the surface chlorophyll-a concentration is the lowest during this season, approximately 67.2% of the study area is characterized by a high chlorophyll-a concentration (>0.4 mg m⁻³) at the SCM, and the SCM occurs at deeper depths in spring than in the other seasons (Table 3). The second multivariate EOF mode (which accounts for 22% of the total variance) of the chlorophyll-a concentration at the SCM also captures the basin-wide high concentration of chlorophyll-a at the SCM during spring (figure not shown). The depth of the 26 °C isotherm also occurs at deeper depths (~71.43 m) in spring than in the other seasons (Table 3). Furthermore, a downwelling gyre is a prominent feature along the western side of the bay in spring (Babu et al., 2003; Vinayachandran et al., 1996). This downwelling

gyre can lower the thermocline, causing the SCM to occur at a deeper depth at this location. Although a deep thermocline is not favorable for a high concentration of chlorophyll-a at the SCM, an excessively deep euphotic depth (>150 m) during spring enables the high chlorophyll-a concentration at the SCM to cover more area than during the other seasons (Figs. 4a3–d3).

3.2.3. Eastern equatorial Indian Ocean

The absence of inputs from continental rivers might be the reason for the low concentrations of chlorophyll-a at both the surface and the SCM in the eastern equatorial Indian Ocean compared with those in the Bay of Bengal throughout the year (Figs. 3–4). On the other hand, the presence of a negative wind stress curl (Fig. 5g) and downwelling Kelvin waves (Yu et al., 1991; Schott and McCreary, 2001; Kumari et al., 2018) deepen the thermocline, which is unfavorable for the upwelling of subsurface nutrients to the surface, and thus, these conditions are also responsible for the low chlorophyll-a concentrations at both the surface and the SCM, as is evident from the negative correlation between the depth of the thermocline and the concentration of chlorophyll-a at the SCM (Table 2). A deep thermocline might also sustain the increased depth of the SCM (70 to 100 m) in the eastern equatorial Indian Ocean relative to that in the Bay of Bengal (Fig. 4). However, the EOF decomposition modes (chlorophyll-a concentrations at the surface and SCM) reflect a patch of high chlorophyll-a on the eastern side of the eastern equatorial Indian Ocean (within the Indonesia dome) during summer and early autumn (Figs. 5a, 6a). The variability of the dominant EOF mode and corresponding PC demonstrates the uplift of the thermocline (negative variability) due to upward Ekman pumping (positive variability) (Figs. 5f–g, 6d–e). Moreover, the (easterly) zonal wind stress anomaly plays an important role in this regard (Saji and Yamagata, 2003; Gonaduwage et al., 2019; Huang et al., 2019), as is evident from the high correlation ($r = 0.50$, Table 2) between the concentration of chlorophyll-a at the SCM and the zonal wind stress. The significant positive relationship between the SSS and turbidity and the surface chlorophyll-a concentration further suggest that highly saline turbid water might originate from the subsurface (Table 2). Thus, the uplift of the thermocline transports cold, nutritious, and highly saline water to the surface, shallowing the MLD and enhancing the concentrations of chlorophyll-a at the surface and SCM within the Indonesia dome. Notably, PO_4^{3-} is more correlated than NO_3^- with the chlorophyll-a concentrations at both the surface and the SCM in the Indonesia dome (Tables 1–2).

4. Discussion

This study provides a comprehensive investigation of the seasonal variations in the spatial and vertical distributions of chlorophyll-a in the Bay of Bengal and the eastern equatorial Indian Ocean. High concentrations of chlorophyll-a at the surface and in the subsurface (at the SCM) within the northern Bay of Bengal, especially in the GBM River estuary and the Irrawaddy River estuary, are greatly influenced by riverine nutrient inputs. However, a prominent river system (the Krishna–Godavari) flows into the western Bay of Bengal and does not govern the concentrations of chlorophyll-a at the surface and SCM, as nutrients from the Arabian Sea and coastal upwelling dominate over this river flow, as is evidenced by the presence of high salinity and the northward-flowing surface current (Fig. 8c). The strong southwesterly wind-mediated Ekman drift causes this coastal upwelling along the western boundary (zonal wind stress in Table 1, Figs. 5f–g, 6d–e), and a similar wind-driven surface current brings water from the Arabian Sea into the Bay of Bengal (Vinayachandran et al., 1999; Wijesekera et al., 2016; Thushara

et al., 2019). Although uplift of the thermocline shallows the depth of the SCM in the entire western part of the Bay of Bengal during summer and early autumn, deepening of the thermocline increases the depth of the SCM and reduces the concentration of chlorophyll-a at the SCM along the eastern side of the Bay of Bengal and eastern equatorial Indian Ocean (Figs. 4a1–d1, 4a2–d2).

Although the basin-wide mean concentration of chlorophyll-a at the SCM is higher during summer (1.09 mg m^{-3}) and autumn (1.01 mg m^{-3}) than during winter and spring, the surface area covered by a high concentration of chlorophyll-a at the SCM is maximal in spring (Table 3, Fig. 10). Moreover, the euphotic depth is shallower during summer and autumn than in the other seasons due to the tremendous volume of monsoonal precipitation and river discharge (Kumar et al., 2010). The euphotic depth is also shallow in winter due to residual monsoonal riverine water. However, in spring, the river discharge of suspended sediment decreases drastically, and eventually, the turbidity of the seawater diminishes (Gomes et al., 2000; Milliman and Farnsworth, 2011). The presence of comparatively high-salinity water also supports the evidence of reduced river discharge during spring compared with other seasons (see the salinity contours in Fig. 11). Lower turbidity allows sunlight to penetrate to deeper depths (euphotic depth > 150 m) (third row in Fig. 4) throughout the spring, resulting in high chlorophyll-a concentrations at the SCM across the bay. Due to the vast input of continental turbid water and suspended phytoplankton, the euphotic depth is shallow in the northern Bay of Bengal, but it deepens latitudinally southward as the turbidity decreases and is deepest in the eastern equatorial Indian Ocean (third row in Fig. 4 and vertical section along 88°E longitude in Fig. 11).

The MLD remains shallow throughout the northern Bay of Bengal (Fig. 12) owing to the freshwater-mediated haline stratification being stronger than that in the southern bay (Fig. 9), as was reported in an earlier study (Chaitanya et al., 2014; Akhil et al., 2014). Hence, the persistent high chlorophyll-a concentration and shallow MLD exhibit an inverse correlation ($r = -0.48$) in this region (Table 1). Although mixing is thought to be conducive to transporting nutrients into the surface layer, in the offshore areas, including the southern Bay of Bengal and the eastern equatorial Indian Ocean, a deep MLD (25 to 45 m) (Fig. 12) is observed throughout the year in conjunction with low surface chlorophyll-a concentrations. Hence, the MLD is not significantly correlated with the surface chlorophyll-a concentration in the Bay of Bengal (Table 1, Figs. 7e, 12).

The surface chlorophyll-a concentration is higher during summer and autumn than in the other seasons when the SST is positively correlated with the surface chlorophyll-a concentration (Figs. 7h, 12c–d). During spring, the highest SST (29 to 31°C) (Fig. 12b) generates strong thermal stratification (Shenoi et al., 2002) and reduces the concentration of surface chlorophyll-a in the Bay of Bengal (Narvekar and Kumar, 2014), which is analogous to the current study region (Fig. 12b). More specifically, the SST and surface chlorophyll-a concentration are positively correlated ($r = 0.71$) in the northern bay, negatively correlated ($r = -0.83$) within the Indonesia dome, and not significantly correlated in the remaining regions (Table 1). Therefore, the spatiotemporally variable relationship between the SST and surface chlorophyll-a concentration suggests that the latter does not always depend on the former in the Bay of Bengal.

During summer and autumn, two eddy-like features are revealed by the vertical distribution of chlorophyll-a (as well as by other studies, e.g., Kumar et al., 2004, 2010; Narvekar and Kumar, 2006; Nuncio and Kumar, 2012: one is in the southern Bay of Bengal (approximately 8 – 9°N latitude), and the other is in the northern Bay of Bengal (approximately 18 – 19.5°N latitude)

Table 3

Basin mean of chlorophyll-a concentration of SCM and associated parameters during different seasons in the study domain.

Parameters	Unit	Winter	Spring	Summer	Autumn
Chlorophyll-a concentration at SCM	mg m ⁻³	0.69	0.58	1.09	1.01
Surface area of SCM (>0.4 mg m ⁻³)	%	40.3	67.2	30.9	40.9
Temperature at SCM depth	°C	26.07	25.81	26.38	26.44
Salinity at SCM depth	unitless	34.48	34.64	34.46	34.41
Nitrate at SCM depth	mmol m ⁻³	3.59	4.11	5.58	4.13
Phosphate at SCM depth	mmol m ⁻³	0.35	0.46	0.45	0.36
Depth of SCM	meter	65.84	68.02	63.35	61.22
Depth of 26 °C isotherm	meter	69.50	71.43	67.74	65.09

(Fig. 11c–d). These eddies are also discernible from the depth of the 26 °C isotherm (see the contours in Figs. 11c–d). This eddy-like upward pumping might help to uplift the SCM depth by 10 to 20 m during summer and autumn relative to that during the other seasons, thereby demonstrating the role of eddies in uplifting the thermocline and thus shoaling the depth of the SCM.

The depth of the SCM is shallow in the northern Bay of Bengal and becomes deeper latitudinally southward, and it is the deepest in the eastern equatorial Indian Ocean (second row in Fig. 4). The depth of the SCM shoals more in the western part of the bay than in the eastern part during summer and autumn. However, the depth of the SCM is deep during winter and reaches the greatest depth in spring throughout the bay. The spatial and temporal distributions of the 26 °C isotherm is similar to those of the depth of the SCM (second row in Fig. 4). The depth of the former follows (within ±5 m) that of the latter, as is observed from the north-south vertical section along 88°E longitude (Fig. 11). The temperature at the SCM varies seasonally between 25.81 and 26.44 °C (Table 3). This indicates that the 26±0.5°C thermocline temperature always follows the depth of the SCM. Therefore, the depth of the 26 °C isotherm can be considered a proxy of the depth of the SCM in the Bay of Bengal and the eastern equatorial Indian Ocean.

5. Conclusions

To date, a complete framework of the dominant processes responsible for the seasonal variation in the concentration of chlorophyll-a at both the surface and the SCM in the Bay of Bengal has not been presented, and thus, this study attempts to comprehensively address this issue. Both external factors, e.g., river inputs, wind forcing, and inflow from the adjacent Arabian Sea, and internal oceanic dynamics, e.g., Ekman pumping, coastal upwelling, variation in the euphotic depth, and thermocline dynamics, regulate the concentration of chlorophyll-a at both the surface and the SCM.

Five potential zones of high chlorophyll-a concentrations at the surface and at the SCM are explored in the current study: along the GBM River estuary, the Irrawaddy River estuary, along the western coast of the Bay of Bengal, the Sri Lanka dome, and the Indonesia dome. Additionally, the entire western part of the southern Bay of Bengal is characterized by a high concentration of chlorophyll-a at the SCM during summer and early autumn, and this newly identified high-concentration area could be a potential source of productivity in the Bay of Bengal.

The GBM and Irrawaddy River systems are the dominant suppliers of nutrients along the estuaries and ultimately enhance the chlorophyll-a concentration both at the surface and in the subsurface. The southwesterly wind-induced positive wind stress curl uplifts the thermocline layer, which enriches the concentration of chlorophyll-a at the SCM in the western Bay of Bengal during summer and early autumn. Moreover, the southwesterly along-shore wind induces coastal upwelling driven by Ekman transport within the Sri Lanka dome and along the western coast of the Bay of Bengal during these seasons. Hence, southwesterly monsoonal

winds exert strong controls over the internal processes in this bay such as thermocline dynamics, coastal upwelling, and Ekman pumping, and increase the concentration of chlorophyll-a at the SCM throughout the whole western part of the Bay of Bengal.

The surface area covered by a high concentration of chlorophyll-a (> 0.4 mg m⁻³) at the SCM is greater during spring than in other seasons due to the comparatively deep euphotic depth during the former. The favorable temperature at the SCM is approximately 26±0.5°C, and thus, the depth of the 26 °C isotherm can be considered a proxy of the depth of the SCM. In addition, the MLD does not significantly control the concentration of surface chlorophyll-a, especially in the offshore areas. The SST also shows a spatiotemporally variable relationship with surface chlorophyll-a, and the surface chlorophyll-a concentration does not always correlate with the SST in this bay.

CRedit authorship contribution statement

K.M. Azam Chowdhury: Conceptualization, Data curation, Formal analysis, Software, Writing – original draft, Editing. **Wen-sheng Jiang:** Supervision, Writing – review & Editing. **Guimei Liu:** Supervision, Funding acquisition. **Md. Kawser Ahmed:** Supervision. **Shaila Akhter:** Investigation, Visualization.

Declaration of competing interest

The authors declare that they have no known competing financial interests or personal relationships that could have appeared to influence the work reported in this paper.

Acknowledgments

This study was conducted using E.U. Copernicus Marine Service Information (CMES), WOA and ERA5 data. The gratitude extends to the Marine Scholarship of China, China Scholarship Council for international student (CSC, Grant no. 2017SOA016552) and National Marine Environmental Forecasting Center, Beijing, China for providing financial support to do this research. We thank Nur Uddin Md Khaled Chowdhury for editing an older version of this manuscript. We also thank reviewers and editor.

References

- Akhil, V.P., Durand, F., Lengaigne, M., Vialard, J., Keerthi, M.G., Gopalakrishna, V.V., Deltel, C., Papa, F., de Boyer Montégut, C., 2014. A modeling study of the processes of surface salinity seasonal cycle in the Bay of Bengal. *J. Geophys. Res. Oceans* 119 (6), 3926–3947. <http://dx.doi.org/10.1002/2013JC009632>.
- Akhter, S., Qiao, F., Wu, K., Yin, X., Chowdhury, K.M.A., Chowdhury, N.U.M.K., 2021. Seasonal and long-term sea-level variations and their forcing factors in the northern Bay of Bengal: A statistical analysis of temperature, salinity, wind stress curl, and regional climate index data. *Dyn. Atmos. Oceans* 95, 101239. <http://dx.doi.org/10.1016/j.dynatmoce.2021.101239>.
- Anderson, G.C., 1969. Subsurface chlorophyll maximum in the northeast Pacific Ocean. *Limnol. Oceanogr.* 14, 386–391. <http://dx.doi.org/10.4319/lo.1969.14.3.0386>.

- Aumont, O., Éthé, C., Tagliabue, A., Bopp, L., Gehlen, M., 2015. PISCES-v2: an ocean biogeochemical model for carbon and ecosystem studies. *Geosci. Model Dev. Discuss.* 8 (2).
- Babu, M.T., Sarma, Y.V.B., Murty, V.S.N., Vethamony, P., 2003. On the circulation in the Bay of Bengal during northern spring inter-monsoon (March–April 1987). *Deep Sea Res. II* 50, 855–865. [http://dx.doi.org/10.1016/S0967-0645\(02\)00609-4](http://dx.doi.org/10.1016/S0967-0645(02)00609-4).
- Baldry, K., Strutton, P.G., Hill, N.A., Boyd, P.W., 2020. Subsurface chlorophyll-a maxima in the southern ocean. *Front. Mar. Sci.* 7, 671. <http://dx.doi.org/10.3389/fmars.2020.00671>.
- Baliarsingh, S.K., Lotliker, A.A., Sahu, K.C., Kumar, S.T., 2015. Spatio-temporal distribution of chlorophyll-a in relation to physico-chemical parameters in coastal waters of the northwestern Bay of Bengal. *Environ. Monit. Assess.* 187, 481. <http://dx.doi.org/10.1007/s10661-015-4660-x>.
- Bhushan, R., Bikina, S., Chatterjee, J., Singh, S.P., Goswami, V., Thomas, L.C., Sudheer, A.K., 2018. Evidence for enhanced chlorophyll-a levels in the Bay of Bengal during early north-east monsoon. *J. Oceanogr. Mar. Sci.* 9 (2), 15–23. <http://dx.doi.org/10.5897/JOMS2017.0144>.
- Bjornsson, H., Venegas, S.A., 1997. A Manual for EOF and SVD Analyses of Climatic Data. CCGCR Report No. 97-1, p. 52.
- [dataset], Bonjean, F., Lagerlof, G.S.E., 2002. Diagnostic model and analysis of the surface currents in the Tropical Pacific Ocean. *J. Phys. Oceanogr.* 32, 2938–2954.
- Bricaud, A., Bosc, E., Antoine, D., 2002. Algal biomass and sea surface temperature in the Mediterranean Basin. *Remote Sens. Environ.* 81, 163–178. [http://dx.doi.org/10.1016/S0034-4257\(01\)00335-2](http://dx.doi.org/10.1016/S0034-4257(01)00335-2).
- Brown, Z.W., Lowry, K.E., Palmer, M.A., van Dijken, G.L., Mills, M.M., Pickart, R.S., Arrigo, K.R., 2015. Characterizing the subsurface chlorophyll a maximum in the Chukchi Sea and Canada Basin. *Deep Sea Res. II* 118, 88–104. <http://dx.doi.org/10.1016/j.dsr.2.2015.02.010>.
- Chaitanya, A.V.S., Lengaige, M., Vialard, J., Gopalakrishna, V.V., Durand, F., Kranthikumar, C., Amritash, S., Suneel, V., Papa, F., Ravichandran, M., 2014. Salinity measurements collected by fishermen reveal a “River in the Sea” flowing along the eastern coast of India. *Bull. Am. Meteorol. Soc.* 95, 1897–1908. <http://dx.doi.org/10.1175/BAMS-D-12-00243.1>.
- Chowdhury, K.M.A., Jiang, W.S., Liu, G.M., Ahmed, M.K., Chowdhury, N.M.K., Chowdhury, S.M.B., 2019. Formation and types of thermal inversion in the Bay of Bengal, CLIVAR Exchanges. Special Issue: CLIVAR-FIO Summer Course on Past, Present and Future Sea Level Changes. 76, pp. 20–23.
- Chowdhury, K.M.A., Mahub-E-Kibria, A.S.M., Akhter, S., Chowdhury, N.M.K., Mithu, M.M., 2017. Variation of water column density in the Bay of Bengal aquatic ecosystem. *Int. J. Fish. Aquat. Stud.* 5 (6), 34–40.
- [dataset], Copernicus Marine In Situ Tac, 2020. For Global Ocean-Delayed Mode in-situ Observations of surface (drifters and HFR) and sub-surface (vessel-mounted ADCPs) water velocity. Quality Information Document (QUID). <http://dx.doi.org/10.13155/41256>, CMEMS-INS-QUID-013-044.
- De Viron, O., Panet, I., Diamant, M., 2006. Extracting low frequency climate signal from GRACE data. *eEarth Discuss* 1 (1), 21–36. <https://hal.archives-ouvertes.fr/hal-00330772/>.
- [dataset], Doron, M., Babin, M., Mangin, A., Fanton d’Andon, O., 2006. Estimation of light penetration, and horizontal and vertical visibility in oceanic and coastal waters from surface reflectance. *J. Geophys. Res.* 112, C06003. <http://dx.doi.org/10.1029/2006JC004007>.
- Enfield, D.B., Mestas-Nuñez, A.M., 1999. Multiscale variabilities in global sea surface temperatures and their relationships with tropospheric climate patterns. *J. Clim.* 12, 2719–2733. [http://dx.doi.org/10.1175/1520-0442\(1999\)012<2719:MVIGSS>2.0.CO;2](http://dx.doi.org/10.1175/1520-0442(1999)012<2719:MVIGSS>2.0.CO;2).
- [dataset], European Centre for Medium-range Weather Forecast (ECMWF), 2011. The ERA-Interim reanalysis dataset, Copernicus Climate Change Service (C3S). Available from <https://www.ecmwf.int/en/forecasts/datasets/archivedatasets/reanalysis-datasets/era-interim>. (Accessed 28 July 2019).
- Falkowski, P.G., Oliver, M.J., 2007. Mix and match: how climate selects phytoplankton. *Nat. Rev. Microbiol.* 5, 813–819. <http://dx.doi.org/10.1038/nrmicro1751>.
- Fennel, K., Boss, E., 2003. Subsurface maxima of phytoplankton and chlorophyll: Steady-state solutions from a simple model. *Limnol. Oceanogr.* 48, 1521–1534. <http://dx.doi.org/10.4319/lo.2003.48.4.1521>.
- Fluteau, F., Ramstein, G., Besse, J., 1999. Simulating the evolution of the Asian and African monsoons during the past 30 Myr using an atmospheric general circulation model. *J. Geophys. Res. Atmos.* 104 (D10), 11995–12018. <http://dx.doi.org/10.1029/1999JD900048>.
- Furuya, K., 1990. Subsurface chlorophyll maximum in the tropical and subtropical western Pacific Ocean: Vertical profiles of phytoplankton biomass and its relationship with chlorophyll-a and particulate organic carbon. *Mar. Biol.* 107, 529–539. <http://dx.doi.org/10.1007/BF01313438>.
- García, H.E., Locarnini, R.A., Boyer, T.P., Antonov, J.I., Baranova, O.K., Zweng, M.M., Reagan, J.R., Johnson, D.R., 2014. *World Ocean Atlas 2013, Volume 4: Dissolved Inorganic Nutrients (phosphate, nitrate, silicate)*. S. Levitus, Ed., A. Mishonov Technical Ed.; NOAA Atlas NESDIS. 76, p. 25.
- Girishkumar, M.S., Ravichandran, M., McPhaden, M.J., 2013. Temperature inversions and their influence on the mixed layer heat budget during winters of 2006–2007 and 2007–2008 in the Bay of Bengal: temperature inversion in the Bay of Bengal. *J. Geophys. Res. Oceans* 118 (5), 2426–2437. <http://dx.doi.org/10.1002/jgrc.20192>.
- Gomes, H.R., Goes, J.L., Saino, T., 2000. Influence of physical processes and freshwater discharge on the seasonality of phytoplankton regime in the Bay of Bengal. *Cont. Shelf Res.* 20, 313–330. [http://dx.doi.org/10.1016/S0278-4343\(99\)00072-2](http://dx.doi.org/10.1016/S0278-4343(99)00072-2).
- Gonaduwage, L.P., Chen, G., McPhaden, M.J., Priyadarshana, T., Huang, K., Wang, D., 2019. Meridional and zonal eddy-induced heat and salt transport in the bay of Bengal and their seasonal modulation. *J. Geophys. Res. Oceans* 124, 8079–8101. <http://dx.doi.org/10.1029/2019JC015124>.
- Gong, X., Jiang, W., Wang, L., Gao, H., Boss, E., Yao, X., Kao, S.J., Shi, J., 2017. Analytical solution of the nitracline with the evolution of subsurface chlorophyll maximum in stratified water columns. *Biogeosciences* 14, 2371–2386. <http://dx.doi.org/10.5194/bg-14-2371-2017>.
- Gopalakrishna, V.V., Murty, V.S.N., Sengupta, D., Shenoy, S., Araligid, N., 2002. Upper ocean stratification and circulation in the northern Bay of Bengal during southwest monsoon of 1991. *Cont. Shelf Res.* 22 (5), 791–802.
- Han, W., Meehl, G.A., Rajagopalan, B., Fasullo, J.T., Hu, A., Lin, J., Large, W.G., Wang, J., Quan, X.W., Trenary, L.L., Wallcraft, A., Shinoda, T., Yeager, S., 2010. Patterns of Indian Ocean sea-level change in a warming climate. *Nat. Geosci.* 3, 546–550. <http://dx.doi.org/10.1038/ngeo901>.
- Hasan, M.M., Hossain, B.M.S., Alam, M.J., Chowdhury, K.M.A., Al Karim, A., Chowdhury, N.M.K., 2018. The prospects of blue economy to promote Bangladesh into a middle-income country. *Open J. Mar. Sci.* 8, 355–369. <http://dx.doi.org/10.4236/ojms.2018.83019>.
- He, Q., Zhan, H., Cai, S., 2020. Anticyclonic eddies enhance the winter barrier layer and surface cooling in the Bay of Bengal. *J. Geophys. Res. Oceans* 125, <http://dx.doi.org/10.1029/2020JC016524>.
- Huang, K., Wang, D., Han, W., Feng, M., Chen, G., Wang, W., Chen, J., Li, J., 2019. Semiannual variability of middepth zonal currents along 5°N in the eastern Indian ocean: Characteristics and causes. *J. Phys. Oceanogr.* 49, 2715–2729. <http://dx.doi.org/10.1175/JPO-D-19-0089.1>.
- Huang, T., Zhou, F., Tian, D., Zhang, J., 2020. Seasonal variations of meso-eddies in the Bay of Bengal and its adjacent regions. *J. Mar. Sci.* <http://kns.cnki.net/kcms/detail/33.1330.P.20200602.1349.002.html>. (in Chinese).
- Jeffrey, S.W., Mantoura, R.F., Wright, S.W., 1997. Phytoplankton pigments in oceanography: guidelines to modern methods. In: Paris. UNESCO, <http://hdl.handle.net/102.100.100/224308?index=1>.
- Jolliffe, I.T., Trendafilov, N., Uddin, M., 2003. A modified principal component technique based on the LASSO. *J. Comput. Graph. Stat.* 12, 531–547. <http://dx.doi.org/10.1198/1061860032148>.
- Kirk, J.T.O., 1994. Light and Photosynthesis in Aquatic Ecosystems, second ed. Cambridge Univ. Press, Cambridge. <http://www.loc.gov/catdir/toc/cam025/93037395.html>.
- Koné, V., Aumont, O., Lévy, M., Resplandy, L., 2009. Physical and biogeochemical controls of the phytoplankton seasonal cycle in the Indian Ocean: A modeling study. *Geophys. Monogr. Ser.* 185, 147–166.
- Kumar, S.P., Muraleedharan, P.M., Prasad, T.G., Gauns, M., Ramaiah, N., de Souza, S.N., Sardesai, S., Madhupratap, M., 2002. Why is the Bay of Bengal less productive during summer monsoon compared to the Arabian Sea? *Geophys. Res. Lett.* 29 (24), 2235. <http://dx.doi.org/10.1029/2002GL016013>.
- Kumar, S.P., Nuncio, M., Narvekar, J., Kumar, A., Sardesai, S., de Souza, S.N., Gauns, M., Ramaiah, N., Madhupratap, M., 2004. Are eddies nature’s trigger to enhance biological productivity in the Bay of Bengal? *Geophys. Res. Lett.* 31, L07309. <http://dx.doi.org/10.1029/2003GL019274>.
- Kumar, S.P., Nuncio, M., Ramaiah, N., Sardesai, S., Narvekar, J., Fernandes, V., Paul, J.T., 2007. Eddy-mediated biological productivity in the Bay of Bengal during fall and spring intermonsoons. *Deep Sea Res. I* 54, 1619–1640. <http://dx.doi.org/10.1016/j.dsr.2007.06.002>.
- Kumar, S.P., Prasad, T.G., 1999. Formation and spreading of Arabian Sea high-salinity water mass. *J. Geophys. Res.* 104 (C1), 1455–1464. <http://dx.doi.org/10.1029/1998JC900022>.
- Kumar, S.P., Roshin, R.P., Narvekar, J., Kumar, P.K.D., Vivekanandan, E., 2009. Response of the Arabian Sea to global warming and associated regional climate shift. *Mar. Environ. Res.* 68, 217. <http://dx.doi.org/10.1016/j.marenvres.2009.06.010>.
- Kumar, S.P., Roshin, P.R., Narvekar, J., Kumar, P.K.D., Vivekanandan, E., 2010. What drives the increased phytoplankton biomass in the Arabian Sea? *Curr. Sci.* 99 (1), 101–106.
- Kumari, A., Kumar, S.P., Chakraborty, A., 2018. Seasonal and interannual variability in the barrier layer of the bay of Bengal. *J. Geophys. Res. Oceans* 123 (2), 1001–1015. <http://dx.doi.org/10.1002/2017JC013213>.
- Kusche, J., Eicker, A., Forootan, E., 2011. Analysis tools for GRACE and related data sets, theoretical basis. In: Eicker, A., Kusche, J. (Eds.), Presented at: Mass Transport and Mass Distribution in the System Earth, Mayschoss, Germany, 12–16 Sept 2011. In: Lecture Notes from the Summer School of DFG SPP1257 Global Water Cycle: The International Geoscience Programme. IGCP.

- Lévy, M., Shankar, D., André, J.M., Sheno, S.S.C., Durand, F., de Boyer Montégut, C., 2007. Basin-wide seasonal evolution of the Indian Ocean's phytoplankton blooms. *J. Geophys. Res.* 112, C12014. <http://dx.doi.org/10.1029/2007JC004090>.
- Lewis, W.M., Hamilton, S.K., Lasi, M.A., Rodríguez, M., Saunders, J.F., 2000. Ecological determinism on the orinoco floodplain. *Bio. Sci.* 50 (8), 681–692. [http://dx.doi.org/10.1641/0006-3568\(2000\)050\[0681:EDOTOF\]2.0.CO;2](http://dx.doi.org/10.1641/0006-3568(2000)050[0681:EDOTOF]2.0.CO;2).
- Li, G., Ke, Z., Lin, Q., Ni, G., Sheng, P., 2012a. Longitudinal patterns of spring intermonsoon phytoplankton biomass, species compositions and size structure in the Bay of Bengal. *Acta Oceanol. Sin.* 31, 121–128.
- Li, G., Lin, Q., Ni, G., Shen, P., Fan, Y., Huang, L., Tan, Y., 2012b. Vertical patterns of early summer chlorophyll a concentration in the indian ocean with special reference to the variation of deep chlorophyll maximum. *J. Mar. Biol. ID* 801248, 1–6. <http://dx.doi.org/10.1155/2012/801248>.
- Li, X., Roevros, N., Dehairs, F., Chou, L., 2017. Biological responses of the marine diatom Chaetoceros social is to changing environmental conditions: A laboratory experiment. *PLoS One* 12, e0188615. <http://dx.doi.org/10.1371/journal.pone.0188615>.
- [dataset], Locarnini, R.A., Mishonov, A.V., Baranova, O.K., Boyer, T.P., Zweng, M.M., Garcia, H.E., Reagan, J.R., Seidov, D., Weathers, K.W., Paver, C.R., Smolyar, I.V., 2019. World ocean atlas 2018, volume 1: temperature. A. Mishonov, technical editor. NOAA Atlas NESDIS. 81, p. 52.
- Madhu, N.V., Jyothibabu, R., Maheswaran, P.A., John Gerson, V., Gopalakrishnan, T.C., Nair, K.K.C., 2006. Lack of seasonality in phytoplankton standing stock (chlorophyll a) and production in the western Bay of Bengal. *Cont. Shelf Res.* 26, 1868–1883. <http://dx.doi.org/10.1016/j.csr.2006.06.004>.
- Madhupratap, M., Gauns, M., Ramaiah, N., Kumar, S.P., Muraleedharan, P.M., de Sousa, S.N., Sardessai, S., Muraleedharan, U., 2003. Biogeochemistry of the Bay of Bengal: physical, chemical and primary productivity characteristics of the central and western Bay of Bengal during summer monsoon 2001. *Deep Sea Res. II* 50, 881–896. [http://dx.doi.org/10.1016/S0967-0645\(02\)00611-2](http://dx.doi.org/10.1016/S0967-0645(02)00611-2).
- Madhupratap, M., Kumar, S.P., Bhattathiri, P.M.A., Kumar, M.D., Raghukumar, S., Nair, K.K.C., Ramaiah, N., 1996. Mechanism of the biological response to winter cooling in the northeastern Arabian Sea. *Nature* 384, 549–552. <http://dx.doi.org/10.1038/384549a0>.
- Masud-Ul-Alam, M., Khan, M.A.I., Sunny, S.K., Rahman, M.A., Rahman, M.S., Mahmud, M.B., Shaheen, M.A.R., 2020. An exclusive in-situ dataset on physicochemical parameters in the gappy northern Bay of Bengal. *Data Brief* 31, 106024. <http://dx.doi.org/10.1016/j.dib.2020.106024>.
- McCreary, J.P., Kohler, K.E., Hood, R.R., Olson, D.B., 1996. A four-component ecosystem model of biological activity in the Arabian Sea. *Prog. Oceanogr.* 37, 193–240. [http://dx.doi.org/10.1016/S0079-6611\(96\)00005-5](http://dx.doi.org/10.1016/S0079-6611(96)00005-5).
- Milliman, J.D., Farnsworth, K.L., 2011. River Discharge to the Coastal Ocean: A Global Synthesis. Cambridge University Press, Cambridge. <http://dx.doi.org/10.1017/CBO9780511781247>.
- Monterey, G., Levitus, S., 1997. Seasonal Variability of Mixed Layer Depth for the World Ocean. Technical Report, NOAA, Silver Spring, Md.
- Morel, A., Antoine, D., 1994. Heating rate within the upper ocean in relation to its bio-optical state. *J. Phys. Oceanogr.* 24, 1652–1665. [http://dx.doi.org/10.1175/1520-0485\(1994\)024<1652:HRWTUO>2.0.CO;2](http://dx.doi.org/10.1175/1520-0485(1994)024<1652:HRWTUO>2.0.CO;2).
- [dataset], Morel, A., Huot, Y., Gentili, B., Werdell, P.J., Hooker, S.B., Franz, B.A., 2007. Examining the consistency of products derived from various ocean color sensors in open ocean (Case 1) waters in the perspective of a multi-sensor approach. *Remote Sens. Environ.* 111, 69–88. <http://dx.doi.org/10.1016/j.rse.2007.03.012>.
- Muraleedharan, K.R., Jasmine, P., Achuthankutty, C.T., Revichandran, C., Dinesh Kumar, P.K., Anand, P., Rejomon, G., 2007. Influence of basin-scale and mesoscale physical processes on biological productivity in the Bay of Bengal during the summer monsoon. *Prog. Oceanogr.* 72, 364–383. <http://dx.doi.org/10.1016/j.pocean.2006.09.012>.
- Murty, D., McMurtrie, R.E., 2000. The decline of forest productivity as stands age: a model-based method for analysing causes for the decline. *Ecol. Modell.* 134, 185–205. [http://dx.doi.org/10.1016/S0304-3800\(00\)00345-8](http://dx.doi.org/10.1016/S0304-3800(00)00345-8).
- Narvekar, J., Kumar, S.P., 2006. Seasonal variability of the mixed layer in the central Bay of Bengal and associated changes in nutrients and chlorophyll. *Deep Sea Res. I* 53, 820–835. <http://dx.doi.org/10.1016/j.dsr.2006.01.012>.
- Narvekar, J., Kumar, S.P., 2014. Mixed layer variability and chlorophyll a biomass in the Bay of Bengal. *Biogeosciences* 11, 3819–3843. <http://dx.doi.org/10.5194/bg-11-3819-2014>.
- Nouel, L., 2012. Global ocean biogeochemistry hindcast. <https://sextant.ifremer.fr/record/da5e467c-7cbd-4cde-a759-9b29b897c722/>. (Accessed 13 March 2019).
- Nuncio, M., Kumar, S.P., 2012. Life cycle of eddies along the western boundary of the Bay of Bengal and their implications. *J. Mar. Syst.* 94, 9–17. <http://dx.doi.org/10.1016/j.jmarsys.2011.10.002>.
- Nuncio, M., Kumar, S.P., 2013. Evolution of cyclonic eddies and biogenic fluxes in the northern Bay of Bengal. *Biogeosci. Discuss.* 10, 16213–16236. <http://dx.doi.org/10.5194/bgd-10-16213-2013>.
- Patra, P.K., Kumar, M.D., Mahowald, N., Sarma, V.V.S.S., 2007. Atmospheric deposition and surface stratification as controls of contrasting chlorophyll abundance in the North Indian Ocean. *J. Geophys. Res.* 112, C05029. <http://dx.doi.org/10.1029/2006JC003885>.
- Picado, A., Alvarez, I., Vaz, N., Varela, R., Gomez-Gesteira, M., Dias, J.M., 2014. Assessment of chlorophyll variability along the northwestern coast of Iberian Peninsula. *J. Sea Res.* 93, 2–11. <http://dx.doi.org/10.1016/j.seares.2014.01.008>.
- Preisendorfer, R.W., Mobley, C.D., 1988. Principal Component Analysis in Meteorology and Oceanography. Elsevier, Amsterdam, The Netherlands.
- Radhakrishna, K., Bhattathiri, P.M.A., Devassy, V.P., 1978. Primary productivity of the bay of bengal during august-september 1976. *Indian J. Mar. Sci.* 7, 94–98.
- Rangelova, E., 2007. A Dynamic Geoid Model for Canada (Ph.D. thesis). University of Calgary, Department of Geomatics Engineering, Report No. 20261.
- Riley, G.A., 1949. Quantitative ecology of the plankton of the western North Atlantic. *Bull. Bingham Oceanogr. Coll.* 12, 1–169.
- Roseli, N.H., Akhir, M.F., Husain, M.L., Tangang, F., Ali, A., 2015. Water mass characteristics and stratification at the shallow Sunda Shelf of southern South China Sea. *Open J. Mar. Sci.* 05, 455–467. <http://dx.doi.org/10.4236/ojms.2015.54036>.
- Saji, N.H., Yamagata, T., 2003. Structure of SST and surface wind variability during indian ocean dipole mode events: COADS observations. *J. Clim.* 16, 2735–2751. [http://dx.doi.org/10.1175/1520-0442\(2003\)016<2735:SOSASW>2.0.CO;2](http://dx.doi.org/10.1175/1520-0442(2003)016<2735:SOSASW>2.0.CO;2).
- Sarang, R.K., Nayak, S., Panigrahy, R.C., 2008. Monthly variability of chlorophyll and associated physical parameters in the southwest Bay of Bengal water using remote sensing data. *Indian J. Mar. Sci.* 37 (3), 256–266.
- Sathyendranath, S., Gouveia, A.D., Shetye, S.R., Ravindran, P., Platt, T., 1991. Biological control of surface temperature in the Arabian Sea. *Nature* 349, 54–56. <http://dx.doi.org/10.1038/349054a0>.
- Schott, F., McCreary, J., 2001. The monsoon circulation of the Indian Ocean. *Prog. Oceanogr.* 51, 1–123.
- Sengupta, D., Bharath Raj, G.N., Sheno, S.S.C., 2006. Surface freshwater from bay of bengal runoff and indonesian throughflow in the tropical indian ocean. *Geophys. Res. Lett.* 33, L22609. <http://dx.doi.org/10.1029/2006GL027573>.
- Shankar, D., McCreary, J.P., Han, W., Shetye, S.R., 1996. Dynamics of the East India Coastal Current: 1. Analytic solutions forced by interior Ekman pumping and local alongshore winds. *J. Geophys. Res.* Oceans 101 (C6), 13975–13991. <http://dx.doi.org/10.1029/96JC00559>.
- Shee, A., Sil, S., Gangopadhyay, A., Gawarkiewicz, G., Ravichandran, M., 2019. Seasonal evolution of oceanic upper layer processes in the northern Bay of Bengal following a single Argo float. *Geophys. Res. Lett.* 46 (10), 5369–5377. <http://dx.doi.org/10.1029/2019GL082078>.
- Sheno, S.S.C., Shankar, D., Shetye, S.R., 2002. Differences in heat budgets of the near-surface Arabian Sea and Bay of Bengal: Implications for the summer monsoon. *J. Geophys. Res.* 107 (C6), 3052. <http://dx.doi.org/10.1029/2000JC000679>.
- Shetye, S.R., Gouveia, A.D., Shankar, D., Sheno, S.S.C., Vinayachandran, P.N., Sundar, D., Michael, G.S., Nampoothiri, G., 1996. Hydrography and circulation in the western Bay of Bengal during the northeast monsoon. *J. Geophys. Res.* 101 (C6), 14011–14025. <http://dx.doi.org/10.1029/95JC03307>.
- Shetye, S.R., Gouveia, A.D., Sheno, S.S.C., Sundar, D., Michael, G.S., Nampoothiri, G., 1993. The western boundary current of the seasonal subtropical gyre in the bay of bengal. *J. Geophys. Res.* Oceans 98, 945–954. <http://dx.doi.org/10.1029/92JC02070>.
- Shetye, S.R., Sheno, S.S.C., Gouveia, A.D., Michael, G.S., Sundar, D., Nampoothiri, G., 1991. Wind-driven coastal upwelling along the western boundary of the Bay of Bengal during the southwest monsoon. *Cont. Shelf Res.* 11, 1397–1408. [http://dx.doi.org/10.1016/0278-4343\(91\)90042-5](http://dx.doi.org/10.1016/0278-4343(91)90042-5).
- Steiner, N.S., Sou, T., Deal, C., Jackson, J.M., Jin, M., Popova, E., Williams, W., Yool, A., 2016. The future of the subsurface chlorophyll-a maximum in the Canada basin—A model intercomparison. *J. Geophys. Res.* Oceans 121, 387–409. <http://dx.doi.org/10.1002/2015JC011232>.
- Suryanarayana, A., Murty, V.S.N., Rao, D.P., 1993. Hydrography and circulation of the bay of bengal during early winter, 1983. *Deep Sea Res. I* 40, 205–217. [http://dx.doi.org/10.1016/0967-0637\(93\)90061-7](http://dx.doi.org/10.1016/0967-0637(93)90061-7).
- Syvitski, J.P.M., Vörösmarty, C.J., Kettner, A.J., Green, P., 2005. Impact of humans on the flux of terrestrial sediment to the global coastal ocean. *Science* 308, 376–380. <http://dx.doi.org/10.1126/science.1109454>.
- Thadathil, P., Gopalakrishna, V.V., Muraleedharan, P.M., Reddy, G.V., Araligid, N., Shenoy, S., 2002. Surface layer temperature inversion in the bay of bengal. *Deep Sea Res. Part I: Ocean. Res. Papers* 49, 1801–1818. [http://dx.doi.org/10.1016/S0967-0637\(02\)00044-4](http://dx.doi.org/10.1016/S0967-0637(02)00044-4).
- Thadathil, P., Muraleedharan, P.M., Rao, R.R., Somayajulu, Y.K., Reddy, G.V., Revichandran, C., 2007. Observed seasonal variability of barrier layer in Bay of Bengal. *J. Geophys. Res.* Oceans 112, C02009. <http://dx.doi.org/10.1029/2006JC00365>.
- Thadathil, P., Suresh, I., Gautham, S., Kumar, S.P., Lengaigane, M., Rao, R.R., Neetu, S., Hegde, A., 2016. Surface layer temperature inversion in the Bay of Bengal: Main characteristics and related mechanisms: surface layer temperature inversion. *J. Geophys. Res.* Oceans 121 (8), 5682–5696. <http://dx.doi.org/10.1002/2016JC011674>.

- Thushara, V., Vinayachandran, P.N., 2016. Formation of summer phytoplankton bloom in the northwestern Bay of Bengal in a coupled physical-ecosystem model. *J. Geophys. Res. Oceans* 121 (12), 8535–8550. <http://dx.doi.org/10.1002/2016JC011987>.
- Thushara, V., Vinayachandran, P.N.M., Matthews, A.J., Webber, B.G.M., Queste, B.Y., 2019. Vertical distribution of chlorophyll in dynamically distinct regions of the southern Bay of Bengal. *Biogeosciences* 16, 1447–1468. <http://dx.doi.org/10.5194/bg-16-1447-2019>.
- Trombetta, T., Vidussi, F., Mas, S., Parin, D., Simier, M., Mostajir, B., 2019. Water temperature drives phytoplankton blooms in coastal waters. *PLoS One* 14, e0214933. <http://dx.doi.org/10.1371/journal.pone.0214933>.
- Vinayachandran, P.N., 2004. Biological response of the sea around Sri Lanka to summer monsoon. *Geophys. Res. Lett.* 31, L01302. <http://dx.doi.org/10.1029/2003GL018533>.
- Vinayachandran, P.N., 2005. Bifurcation of the east india coastal current east of sri lanka. *Geophys. Res. Lett.* 32, L15606. <http://dx.doi.org/10.1029/2005GL022864>.
- Vinayachandran, P.N., Saji, N.H., Yamagata, T., 1999. Response of the equatorial Indian Ocean to an unusual wind event during 1994. *Geophys. Res. Lett.* 26, 1613–1616. <http://dx.doi.org/10.1029/1999GL900179>.
- Vinayachandran, P.N., Shankar, D., Vernekar, S., Sandeep, K.K., Amol, P., Neema, C.P., Chatterjee, A., 2013. A summer monsoon pump to keep the Bay of Bengal salty. *Geophys. Res. Lett.* 40, 1777–1782. <http://dx.doi.org/10.1002/grl.50274>.
- Vinayachandran, P.N., Shetye, S.R., Sengupta, D., Gadgil, S., 1996. Forcing mechanisms of the Bay of Bengal circulation. *Curr. Sci.* 71, 753–763.
- Wang, J., Tang, D., Sui, Y., 2010. Winter phytoplankton bloom induced by subsurface upwelling and mixed layer entrainment southwest of Luzon Strait. *J. Mar. Syst.* 83, 141–149. <http://dx.doi.org/10.1016/j.jmarsys.2010.05.006>.
- Webster, P.J., 1987. The elementary monsoon. In: Fein, J.S., Stephens, P.L. (Eds.), *Monsoons*. Wiley-Interscience, New York, pp. 3–32.
- Wijesekera, H.W., Shroyer, E., Tandon, A., Ravichandran, M., Sengupta, D., Jinadasa, S.U.P., Fernando, H.J.S., Agrawal, N., Arulananthan, K., Bhat, G.S., Baumgartner, M., Buckley, J., Centurioni, L., Conry, P., Farrar, J.T., Gordon, A.L., Hormann, V., Jarosz, E., Jensen, T.G., Johnston, S., Lankhorst, M., Lee, C.M., Leo, L.S., Lozovatsky, I., Lucas, A.J., Mackinnon, J., Mahadevan, A., Nash, J., Omand, M.M., Pham, H., Pinkel, R., Rainville, L., Ramachandran, S., Rudnick, D.L., Sarkar, S., Send, U., Sharma, R., Simmons, H., Stafford, K.M., St. Laurent, L., Venayagamoorthy, K., Venkatesan, R., Teague, W.J., Wang, D.W., Waterhouse, A.F., Weller, R., Whalen, C.B., 2016. ASIRI: An ocean-atmosphere initiative for bay of bengal. *Amer. Meteor. Soc.* 97, 1859–1884. <http://dx.doi.org/10.1175/BAMS-D-14-00197.1>.
- Wolken, J.J., Mellon, A.D., Greenblatt, C.L., 1955. Environmental Factors affecting growth and chlorophyll synthesis. *J. Protozoal.* 2, 89–96.
- Yu, L., O'Brien, J.J., Yang, J., 1991. On the remote forcing of the circulation in the Bay of Bengal. *J. Geophys. Res.* 96 (C11), 20449–20454. <http://dx.doi.org/10.1029/91JC02424>.
- Zhang, W.Z., Wang, H., Chai, F., Qiu, G., 2016. Physical drivers of chlorophyll variability in the open South China Sea: Chlorophyll variability in the SCS. *J. Geophys. Res. Oceans* 121 (9), 7123–7140. <http://dx.doi.org/10.1002/2016JC011983>.
- [dataset], Zweng, M.M., Reagan, J.R., Seidov, D., Boyer, T.P., Locarnini, R.A., Garcia, H.E., Mishonov, A.V., Baranova, O.K., Weathers, K.W., Paver, C.R., Smolyar, I.V., 2019. *World ocean atlas 2018, volume 2: Salinity*. A. Mishonov, technical editor, NOAA Atlas NESDIS. 82, p. 50.